

Review

Diffusion Bonding and Transient Liquid Phase (TLP) Bonding of Type 304 and 316 Austenitic Stainless Steel—A Review of Similar and Dissimilar Material Joints

Abdulaziz AlHazzaa ^{1,2}  and Nils Haneklaus ^{2,3,*} 

¹ Research Chair for Tribology, Surface, and Interface Sciences (TSIS), Physics and Astronomy Department, College of Science, King Saud University, P.O. Box 2455, Riyadh 11451, Saudi Arabia; aalhazaa@ksu.edu.sa

² King Abdullah Institute Nanotechnology, King Saud University, Riyadh 11451, Saudi Arabia

³ Faculty of Mechanical Engineering, RWTH Aachen University, Eilfschornsteinstr. 18, 52072 Aachen, Germany

* Correspondence: nils.haneklaus@rwth-aachen.de

Received: 20 April 2020; Accepted: 4 May 2020; Published: 8 May 2020



Abstract: Similar and dissimilar material joints of AISI grade 304 (1.4301) and AISI grade 316 (1.4401) austenitic stainless steel by solid state diffusion bonding and transient liquid phase (TLP) bonding are of interest to academia and industry alike. Appropriate bonding parameters (bonding temperature, bonding time, and bonding pressure) as well as suitable surface treatments, bonding atmosphere (usually high vacuum or protective gas) and interlayers are paramount for successful bonding. The three main parameters (temperature, time, and pressure) are interconnected in a strong non-linear way making experimental data important. This work reviews the three main parameters used for solid state diffusion bonding, TLP bonding and to a smaller degree hot isostatic pressing (HIP) of AISI grade 304 and AISI grade 316 austenitic stainless steel to the aforementioned materials (similar joints) as well as other materials, namely commercially pure titanium, Ti-6Al-4V, copper, zircaloy and other non-ferrous metals and ceramic materials (dissimilar joints).

Keywords: diffusion bonding; transient liquid phase bonding; stainless steel; dissimilar joints

1. Introduction

Diffusion bonding is a solid-state welding technique capable of joining similar and dissimilar materials. The process operates on the principle of solid-state diffusion, wherein the atoms of two solid materials intersperse themselves over time at elevated temperature and pressure so that a high-quality bond between the base materials is formed [1]. Solid state diffusion bonding is attractive for the joining of dissimilar materials since the formation of brittle intermetallic compounds (IMCs) as well as chemical segregation and accumulation of residual stress at the bond interface can be relatively low if compared to other welding techniques [2–4]. Compared with other joining techniques, diffusion bonding is expensive and only widespread in aerospace engineering. Besides being able to join dissimilar materials, diffusion bonding can be used for full cross-section joining that may be particularly interesting for holohedral joints, such as internal structures of plate-type heat exchangers [5,6]. Transient liquid phase (TLP) bonding differs from solid-state diffusion bonding in a way that a thin interlayer, that has a lower melting point than the base materials and can melt below the bonding temperature, is placed between the base materials that are to be joined. The interlayer element (or constituent of an alloy interlayer is used) diffuses into the base materials, causing isothermal solidification at the bonding temperature. As a result, a bond that has a higher melting point than the initial TLP bonding

Grade 304 and 316 austenitic stainless steel are diffusion bonded for a number of applications. Most notably these diffusion bonds are used for aerospace applications [15–17], production of plate type heat exchangers or chemical reactors [18–25] and fusion reactors [26–28]. The protective oxide layer on austenitic stainless steel [29] results in good corrosion resistance of the material and makes diffusion bonding it not a trivial manner.

Different review papers on the diffusion bonding of stainless steels exist. Fang et al. [30] as well as Cai et al. [31] provide reviews on solid-state welding of dissimilar metals. Tomashchuk and Sallamand [32] report on joining strategies of titanium alloys and steels. In all three reviews dissimilar diffusion bonding of austenitic stainless steels has a prominent role. Mo et al. [33] further specifically reviewed diffusion bonding between titanium alloys and stainless steels. Gietzelt et al. [34] present a systematic study for diffusion bonding of 304 stainless steel that puts particular focus on the deformation during diffusion welding. In a clever way, cone-shaped samples (“Gietzelt-Cones”) consisting of several layers with slightly different areas were diffusion bonded so that different applied loads could be investigated with one sample diffusion bonded using the same force.

In this work we review similar and dissimilar material diffusion bonding and TLP bonding experiments conducted to join 304 and 316 austenitic stainless steel, including their low-carbon versions 304L, 316L and 316LN as well as the higher carbon variant 316H. Specifically we report on the different bonding parameters (bonding temperature, bonding pressure and bonding time). We further report the selected interlayers. Interlayers are particularly relevant if different materials with different coefficients of thermal expansion are to be joined [35,36]. Although diffusion bonding can be conducted in air [37–40] it is usually conducted in high vacuum or under protective gas atmosphere. We therefore do not explicitly report on the used atmosphere of the reported experiments. Besides the used atmosphere [1], surface treatments [41], sample geometries, furnace design, pre- and post-treatment of samples can have a significant impact on the quality of the diffusion bond. Reporting on all these different factors would go beyond the scope of this work and we thus decided to limit reporting to four factors: type of interlayer, (bonding) temperature, (bonding) time and (bonding) pressure that we found most relevant. We define bonding pressure, bonding temperature and bonding time as the parameters during the actual diffusion bonding process. Figure 2 provides a brief overview of the basic diffusion bonding process and the three reported parameters.

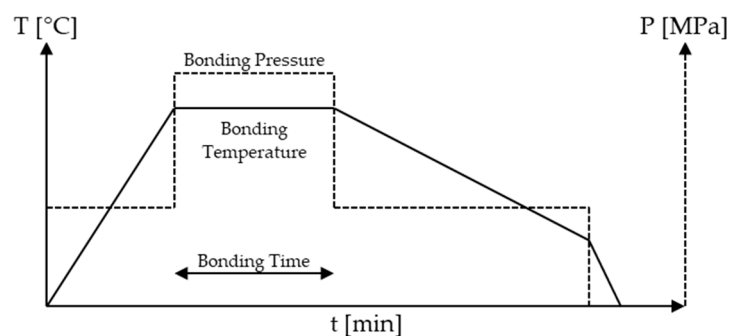


Figure 2. Schematic overview of the reported parameters: bonding pressure, bonding temperature and bonding time in the basic diffusion bonding process.

In the basic diffusion bonding process, as we define it here, samples are fixed at a low pressure and heated with a certain heating rate until the desired bonding temperature is reached. When the desired bonding temperature is reached the pressure will usually be increased to the desired bonding pressure. Both bonding temperature and bonding pressure will be kept constant over the bonding time (sometimes referred to as holding time or soak time). After the defined bonding time, the pressure will usually be reduced (in Figure 2 it was reduced to the initial temperature used to fix the sample) and the temperature is gradually reduced to room temperature.

Fick's first law with the following temperature (T) dependent diffusion coefficient (D):

$$D = D_0 e^{-Q/RT} \quad (1)$$

is usually used to represent the diffusion bonding process (D_0 is the frequency factor, Q the activation energy and R the gas constant). Atomic diffusion across the mating surfaces normally occurs before reaching the defined diffusion bonding temperature and similarly the process of diffusion still occurs while the sample cools down. Therefore, looking at bonding pressures, bonding temperatures and bonding times does provide a good overview, but does not tell the whole story of the conducted experiments. Song et al. [42] provide for instance a two-stage diffusion bonding process for joining 316L with a titanium alloy. In the process samples are first heated to 750 °C and kept there under 30 MPa load for 20 min before moving to the second diffusion bonding stage where samples are diffusion bonded at 900 °C and under 5 MPa pressure for another 30–120 min. Work by Shirzadi and Wallach [43–45] further showed that a temperature gradient perpendicular to the bond plane has a benevolent effect on the final bond quality. Another interesting option is rapid temperature changes that were for instance used by Sheng et al. [46]. It is further relevant to understand if the reported bonding temperature, was measured in the parts (for example by mounting a thermocouple on the sample close to the bond) or the furnace, as these two temperatures can differ significantly from each other.

Besides temperature, actual bonding pressure is challenging to thoroughly report on as well. In the basic diffusion bonding process that was introduced earlier, pressure is applied in a controlled manner using a ram. Not only different constant pressures but also varying the same pressure (“hammering”) can have an effect on the quality of the diffusion bond. This may best be illustrated by works on impulse pressure diffusion bonding (IPDB), where the bonding pressure is increased and decreased several times over the course of the actual diffusion bonding time [47–56]. Diffusion bonding is also performed with vacuum furnaces that do not possess a ram and can thus not apply or control the applied pressure. Akhter et al. [57,58] and Munis et al. [59], for instance, report on diffusion bonding of 316L stainless steel and Zircaloy-4 samples in a vacuum furnace in which pressure was applied by putting the samples in a vice machine for 24 h before the actual heat treatment to introduce plastic deformation on the bonded surfaces. Samples were then wrapped in Kanthal wire that has a lower coefficient of thermal expansion than 316L and Zircaloy-4 so that pressure builds up during heating. Taking advantage of different coefficients of thermal expansion to generate pressure for diffusion bonding is not unusual [60–62] and can be complemented by clamp-like apparatuses that apply compression using screws [63–67]. If the sample geometry allows it, parts can also be press-fitted and put under pressure into a vacuum furnace where they are then diffusion bonded when the temperature is increased [68–70]. If no relevant pressure was applied [67,71–87], the experiments were not reported here since we considered them brazing rather than diffusion bonding using the definitions introduced earlier. In brazing some pressure is often applied to fix the parts so that a definition between brazing and TLP bonding that only relates to applied pressure is not sufficient. An interesting case is for instance the experiments conducted by Xia et al. [88–90] who used a deadweight to apply 0.02 MPa pressure during the whole bonding process, so that these works on joining of 316L stainless steel with titanium and titanium alloy (Ti-6Al-4V) could be considered diffusion bonding studies, or more accurately TLP bonding, since melting interlayers were used that at least partly diffused into the base materials. Since the weight was so little, and more importantly the interlayers did not completely diffuse into the base materials, we did not consider them diffusion bonding or TLP bonding studies in this review. We consequently did also not consider the weight of the upper part of a diffusion bonding sample a dead weight or applied pressure.

It is worth noting that the applied pressure in diffusion bonding is used to bring the base materials closer together, and overcome oxide layers and asperities of the faying surfaces. The applied temperature, as indicated in Equation (1) has by far the largest effect on the diffusion bonding process. Other related diffusion bonding processes such as hybrid friction diffusion bonding (HFDB) of stainless steels [91,92] were also not considered in this review. It can also be argued that sintering is a form of

diffusion bonding small kernels, or diffusion bonding is a form of sintering large plates. We do not argue either way and did not consider sintering experiments of 304 and 316 stainless steels [93–102] in this study.

Rather than being comprehensive, this work aims to provide a focused overview on conducted similar and dissimilar diffusion bonding experiments of grade 304 and grade 316 stainless steel. To reproduce experiments, we strongly recommend reviewing the relevant references to learn about the detailed parameters which were not reported here, such as surface preparations, pre- and post-bonding treatment, that can have a significant impact on the overall quality of the achieved bond.

2. Materials and Methods

For this study more than 1200 papers published by various authors were reviewed using Scopus, Web of Science and Google Scholar. Four factors: interlayer, (bonding) temperature, (bonding) time and bonding (pressure) that we found most relevant were reported from nearly 140 studies. Figure 3 provides an overview of the considered scientific publications on similar and dissimilar diffusion bonding and TLP bonding of 304 and 316 stainless steel over the past 20 years.

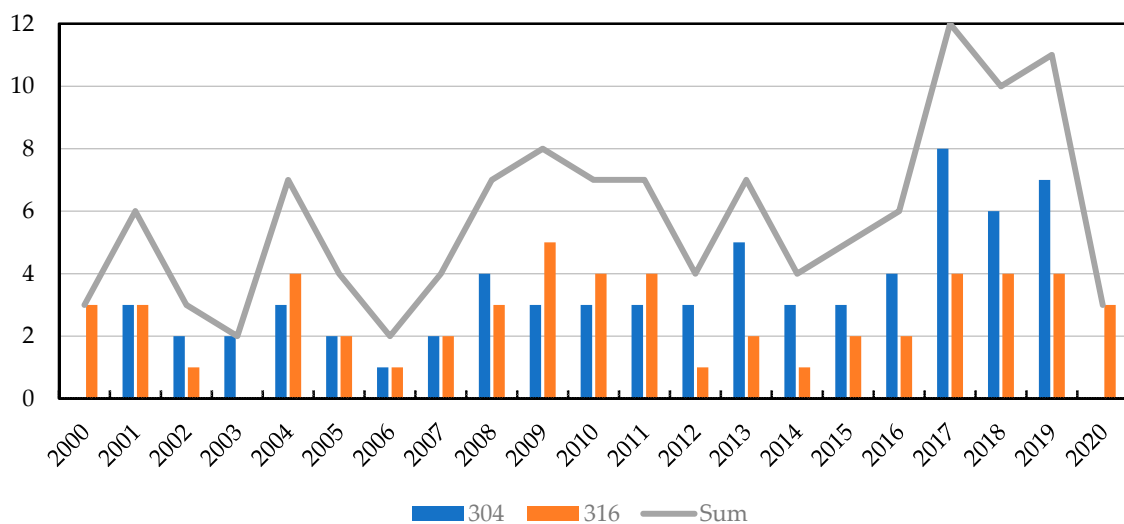


Figure 3. Number of considered scientific publications on similar and dissimilar diffusion bonding and TLP bonding of 304 and 316 stainless steel over the last 20 years.

In detail, we reported the factors recommended by the authors. If the same result would be achieved with different bonding conditions, we would recommend the lower, easier and less costly parameter. If, for instance, the same bond quality, determined by tensile testing, could be achieved at 800 °C and 900 °C ($P = \text{const}$, $t = \text{const}$), then we would recommend using 800 °C. We further placed emphasis on the mechanical strength of the reported diffusion bonds, usually measured with tensile- or shear tests. Depending on the application at hand, other parameters such as deformation not reported here may be equally important to those conducting the experiments.

3. Results and Discussion

3.1. Diffusion Bonding and TLP Bonding of 304 (Similar Joints)

Table 2 provides a brief overview of similar diffusion bonding and TLP bonding studies of 304 stainless steel. Gawde et al. [103] used five interlayers (set-up: 304/Ni/Cu/Ag/Cu/Ni/304) to bond 304 stainless steel rods at a relatively low temperature of 500 °C and very low pressure of 0.1 MPa, that was basically just used to keep the set-up in place. Despite the low bonding temperature and pressure the bonded samples reached tensile strength of 130 MPa before they would rupture at the Ag interface ($UTS\text{-Ag} = 140\text{ MPa}$) indicating incomplete diffusion of the interlayer into the base material.

Table 2. Reported parameters for similar diffusion bonding and TLP bonding of 304.

M1	M2	Interlayer	Temperature	Time	Pressure	Ref.
304	304	Ni-Cu-Ag (2–3; 5; 2–3 μm) ¹	500 °C	120 min	0.1 MPa	[103]
304	304	Cu (50 μm)	950 °C	72 min	0.5 MPa	[107]
304	304	-	1000 °C	60 min	3.5 MPa	[41]
304	304	-	1100 °C	16 min	NR ²	[108]
304	304	Ni (75 μm)	1150 °C	20 min	0.5 MPa	[104]
304	304	Ni (75 μm)	1150 °C	20 min	0.5 MPa	[105]
304	304	-	1175 °C	60 min	15 MPa	[109]
304	304	Co (40 μm)	1180 °C	30 min	0.2 MPa	[106]
304	304	NiB (25 μm)	1200 °C	3 min	9.8 MPa	[110]

¹ Three different interlayer materials: Ni (thickness: 2–3 μm), Cu (thickness 5 μm) and Ag (thickness 2–3 μm) were used. ² NR = not reported.

Much higher mechanical bond strengths were reported by Lamijiri and Ekrami [104] who bonded 304 stainless steel plates of 6 mm thickness using a 75 μm Ni-foil (MBF30, Ni_{4.5}Si_{3.2}B_{0.06}C) achieving shear strength of 532 MPa (78% of the base material experiencing the same heat treatment) after diffusion bonding at 1150 °C for 20 min applying a load of 0.5 MPa. The shear strength could slightly be improved to 552 MPa (81% of the base material experiencing the same heat treatment) through homogenization of the bond at 950 °C for another 180 min. In another work of the same research group from Sharif University of Technology [105] that used the same bonding conditions and discusses the corrosion behavior of these joints, even 83% of the base materials strength could be accomplished. The research group further reported on shear strength of diffusion bonded (1150 °C, 30 min, 0.2 MPa) 304 stainless steel plates using a 40 μm Co-based interlayer [106]. With this set-up a shear strength of up to 90% of the base material was achieved. On average, unhomogenized samples reached roughly 50% of the base materials bond strength and homogenized samples reached 72% of the base materials bond strength (all compared to the base material experiencing the same heat treatment). Other studies listed in Table 2 did unfortunately not report on the mechanical strength of the bond, so it is hard to quantitatively compare the achieved results.

3.2. Diffusion Bonding and TLP Bonding of 316 (Similar Joints)

Table 3 reports on similar diffusion bonding and TLP bonding experiments of 316 stainless steel. Just like similar bonding of 304 stainless steel this is a common process in industry so that the conducted experiments are generally concerned with additional influences or optimizations such as the impact on roll bonding on the diffusion bonding behavior [111] or the investigation of fatigue [112] and corrosion [112] behavior that go beyond “simply” reporting bonding parameters. A comparison is also difficult since most publications did not conduct mechanical tests that generate quantitative results, and if quantitative results are reported they are often not put in perspective by comparing them to the strength of the base material experiencing the same heat treatment.

Yeh and Chuang [113] provide excellent documentation for their study on diffusion bonding of 316 stainless steel rods. The researchers compare diffusion bonding of 316 stainless steel samples with and without interlayer (Dux 65: wt% 23.8 Cr, 5.9 Ni, 1.5 Mo, 1.1 Cu, 0.7 Si, 0.7 Mn, 0.14 N, 0.05 Al, 0.035 P, 0.03 C, 0.002 S, balance Fe) at different surface finishes. With a high surface finish, 99% of the bond strength of the base material could be confirmed through tensile testing (samples still fractured at the bond plane), while samples with lower surface finishes reached 38% of the base materials bond strength. Using the Dux 65 interlayer the diffusion bonds outperformed the base material with high and low surface finish and samples consequently fractured in the base material. These high bond strengths are not unusual and correspond well to the 94% ultimate tensile strength (566 MPa) of the base material reported for the solid-state diffusion bonding without the interlayer of 316L reported by Li et al. [114]. Similar results have also been reported by Mateus et al. [115]: ~550 MPa (also diffusion bonding of 316L without interlayer).

Table 3. Reported parameters for similar diffusion bonding and TLP bonding of 316.

M1	M2	Interlayer	Temperature	Time	Pressure	Ref.
316 ¹	316	Cu-Ti (~1; ~1 µm)	900 °C	10 min	0.9 MPa	[116]
316	316	-	920 °C	240 min	27.6 MPa	[117]
316L	316L	-	1000 °C	30 min	9.8 MPa	[111]
316L	316L	-	1000 °C	120 min	4 MPa	[118]
316L	316L	Ni ² (min. 2 µm)	1000 °C	120 min	6.9 MPa	[119]
316L	316L	Ni ² (6 µm)	1000 °C	120 min	10 MPa	[120]
316	316	Dux 65 (1000 µm)	1027 °C	30 min	7 MPa	[113]
316L	316L	-	1040 °C	60 min	8 MPa	[115]
316H	316H	-	1050 °C	60 min	8 MPa	[121]
316L	316L	-	1050 °C	60 min	10 MPa	[122]
316L	316L	-	1075 °C	300 min	6.4 MPa	[123]
316L	316L	-	1100 °C	180 min	10 MPa	[112,114,124,125]

¹ Metal foam, ² Ni nanoparticles.

3.3. Diffusion Bonding and TLP Bonding of 304 and 316 to Commercially Pure Titanium (cpTi)

Table 4 reports on dissimilar joining by diffusion bonding and TLP bonding of 304 and 316 stainless steel to commercially pure titanium (cpTi). Titanium and its alloys show extraordinary mechanical properties and corrosion resistance. The widespread usage of titanium and its alloys is, however, limited as a result of the relatively high costs. To save costs titanium is frequently joined to more common and cheaper structural materials such as stainless steel, so that the individual components of both materials can be fully exploited and the overall cost of the structures can be reduced. Diffusion bonding and TLP bonding of titanium and titanium alloys finds particularly wide application in aerospace engineering [126] which can explain the relatively large number of experiments conducted and reported in Table 4. Compared with similar diffusion bonding and TLP bonding of 304 and 316, considerably lower temperatures were used.

Table 4. Reported parameters for diffusion bonding and TLP bonding of 304 and 316 to commercially pure titanium (cpTi).

M1	M2	Interlayer	Temperature	Time	Pressure	Ref.
304L	cpTi	Al (120 µm)	650 °C	90 min	3 MPa	[127]
304	cpTi	Al (50–60 µm)	650 °C	120 min	2 MPa	[128]
316L	cpTi	-	677 °C	15 min	5 MPa	[129]
304L	cpTi	-	738 °C	8 min	51 MPa	[130]
316L	cpTi	-	800 °C	15 min	15 MPa	[131]
304	cpTi	-	800 °C	120 min	3 MPa	[132]
304	cpTi	-	820 °C	60 min	NR	[133] ¹
304	cpTi	Ni (0.5–1.1 µm)	850 °C	60 min	NR	[133] ¹
304	cpTi	Ag (50 µm)	850 °C	20 min	8 MPa	[134,135]
304	cpTi	Cu-Zn (100; 100 µm)	850 °C	30 min	NR	[136]
304	cpTi	-	850 °C	120 min	3 MPa	[137]
304	cpTi	Nb–Ni (10, 10 µm)	900 °C	30 min	1 MPa	[138]
304	cpTi	Nb (300 µm)	900 °C	30 min	3 MPa	[139]
304	cpTi	Ni (100 µm)	900 °C	60 min	2 MPa	[140,141]
304	cpTi	Ni (300 µm)	900 °C	60 min	3 MPa	[142]
304	cpTi	Cu (300 µm)	900 °C	60 min	3 MPa	[143]
304	cpTi	Cu (300 µm)	900 °C	90 min	3 MPa	[144]
304	cpTi	Nb (300 µm)	900 °C	120 min	3 MPa	[145]
316	cpTi	Cu (40 µm)	950 °C	50 min	3 MPa	[146]

¹ Gallium assisted diffusion bonding, NR = not reported.

A large number of researchers reported detailed mechanical bond strengths measured using tensile tests for joining of 304 and cpTi so that we can attempt to compare the reported ultimate tensile strengths (UTS) with one another as was done in Table 5. Detailed references of the cited twelve studies are provided to give credit to the research-groups conducting them. Relatively high bond strength ranging from 70% to 100% of the weaker base material cpTi were reported without and with a number of interlayers. The reported UTS of the base material, cpTi Grade 1 and cpTi Grade 2 vary considerably so that we considered the relative bond strength measured in % UTS of the cpTi, that is the weaker base material, as the most relevant criteria. Cu-interlayers of 300 μm thickness seem to accomplish particularly good results. In general, samples with interlayers show higher bond strength than samples that were bonded directly. The study conducted by Shirzadi et al. [133] is an exception to this observation. In this study samples without an interlayer do in fact outperform the samples with a thin 0.5–1.1 μm Ni interlayer. In their study Shirzadi et al. [133] use gallium to remove the oxide layer prior to diffusion bonding so that this can be considered a special case.

Table 5. Comparison of the ultimate tensile strength (UTS) of diffusion bonded and TLP bonded 304 with commercially pure titanium (cpTi) samples.

Study	304	Interlayer	cpTi	UTS of cpTi ¹	UTS of Joint	% UTS of cpTi
Gosh et al. [137]	304	-	Gr 1	319 MPa	222 MPa	70%
Gosh et al. [132]	304	-	Gr 1	319 MPa	242 MPa	76%
Li et al. [138]	304	Nb-Ni (10; 10 μm)	Gr 2	490 MPa	398 MPa	81%
Shirzadi et al. [133] ²	304	Ni (0.5–1.1 μm)	Gr 2	340 MPa	280 MPa	82%
Kundu and Chatterjee [127]	304L	Al (120 μm)	Gr 1	319 MPa	266 MPa	83%
Deng et al. [134]	304	Ag (50 μm)	Gr 2	486 MPa	410 MPa	84%
Deng et al. [135]	304	Ag (50 μm)	Gr 2	486 MPa	421 MPa	87%
Kundu and Chatterjee [145]	304	Nb (300 μm)	Gr 1	319 MPa	287 MPa	90%
Shirzadi et al. [133] ²	304	-	Gr 2	340 MPa	313 MPa	92%
Kundu and Chatterjee [139]	304	Nb (300 μm)	Gr 1	319 MPa	297 MPa	93%
Kundu and Chatterjee [142]	304	Ni (300 μm)	Gr 1	319 MPa	302 MPa	95%
Kundu and Chatterjee [144]	304	Cu (300 μm)	Gr 1	319 MPa	318 MPa	100%
Kundu and Chatterjee [143]	304	Cu (300 μm)	Gr 1	319 MPa	322 MPa	101% ³

¹ As reported by study, ² Gallium assisted diffusion bonding, ³ Sample ruptured in the cpTi base material at a UTS of 101% of the cpTi base material.

3.4. Diffusion Bonding and TLP Bonding of 304 and 316 to Ti-6Al-4V

Besides diffusion bonding and TLP bonding of 304 and 316 stainless steel and cpTi, a large number of publications looked into diffusion bonding of 304 and 316 stainless steel to Ti-6Al-4V (Grade 5). Ti-6Al-4V is the most used titanium alloys that due to its balance (as α - β alloy) has low density and excellent corrosion resistance. Diffusion bonding and TLP bonding parameters are reported in Table 6. Since a large number of researchers reported UTS and shear strength of their experiments, we also directly compared these results (UTS left and shear strength right) in Figure 4. It was noticed that among the 13 papers available that specifically bond 304 to Ti-6Al-4V, ten used interlayers to facilitate the atomic diffusion process and therefore acquire high quality bond strengths. Nevertheless, the solid-state diffusion bonding study by Ghosh et al. [147] achieved with 342 MPa the highest UTS reported for direct bonding of 304 to Ti-6Al-4V. Only the study by Song et al. [42] who joined 316L to Ti-6Al-4V using a Cu-Nb interlayer and a two-step diffusion bonding process mentioned in the introduction, reached a higher value (489 MPa). The reported UTS ranged from as low as 183 MPa [148] to the aforementioned high value reported by Song et al. [42]. The reasons for this may be found in the different user requirements for the bond. Chandrappa et al. [148] who reached the 183 MPa UTS, did for instance conduct joining experiments at a relatively low maximum temperature of 550 $^{\circ}\text{C}$, while all others used bonding temperatures ranging from 750 to 1100 $^{\circ}\text{C}$. With aluminum the researchers further used an interlayer that is notoriously difficult to join using diffusion bonding [149–152]. Reported shear strengths range from as low as 118 MPa to as high as 385 MPa. The highest reported value was again

reached with a combination of 316L and Ti-6Al-4V as well as a Cu-Ni interlayer. The five studies with the highest reported shear strength all used copper interlayers.

Table 6. Reported parameters for diffusion bonding and TLP bonding of 304 to Ti-6Al-4V.

M1	M2	Interlayer	Temperature	Time	Pressure	Ref.
304	Ti-6Al-4V	Al (1,000 μm)	550 $^{\circ}\text{C}$	60 min	12 MPa	[148]
304	Ti-6Al-4V	Ni (200 μm)	750 $^{\circ}\text{C}$	60 min	3 MPa	[153]
304	Ti-6Al-4V	Au (100 μm)	800 $^{\circ}\text{C}$	60 min	5 MPa	[154]
304	Ti-6Al-4V	-	800 $^{\circ}\text{C}$	90 min	3 MPa	[147]
304	Ti-6Al-4V	Ag (60 μm)	800 $^{\circ}\text{C}$	90 min	5 MPa	[155]
304	Ti-6Al-4V	Ni (30 μm)	850 $^{\circ}\text{C}$	10 min	10 MPa	[156]
304	Ti-6Al-4V	Cu (200 μm)	850 $^{\circ}\text{C}$	75 min	4 MPa	[157]
304	Ti-6Al-4V	Ag (5000 μm)	850 $^{\circ}\text{C}$	90 min	5 MPa	[158]
304	Ti-6Al-4V	Cu (60 μm)	870 $^{\circ}\text{C}$	90 min	1 MPa	[159]
316L	Ti-6Al-4V	V-Cu-Co (NR)	880 $^{\circ}\text{C}$	90 min	5 MPa	[160]
316L	Ti-6Al-4V	-	885 $^{\circ}\text{C}$	30 min	5 MPa	[161]
316	Ti-6Al-4V	Cu (50 μm)	900 $^{\circ}\text{C}$	60 min	2 MPa	[162]
304L	Ti-6Al-4V	-	900 $^{\circ}\text{C}$	60 min	4 MPa	[163]
304	Ti-6Al-4V	-	900 $^{\circ}\text{C}$	75 min	14 MPa	[164]
316L	Ti-6Al-4V	Cu-Nb (20; 25 μm)	900 $^{\circ}\text{C}$	90 min	5 MPa	[42]
316L	Ti-6Al-4V	-	950 $^{\circ}\text{C}$	180 min	8 MPa	[165]
304	Ti-6Al-4V	Cu (25 μm)	960 $^{\circ}\text{C}$	60 min	<1 MPa	[166]
304	Ti-6Al-4V	Cu (25 μm)	960 $^{\circ}\text{C}$	60 min	1 MPa	[167]
316L	Ti-6Al-4V	Cu-Ni (100; 50 μm)	1000 $^{\circ}\text{C}$	30 min	2 MPa	[168]
316	Ti-6Al-4V	Cu (50 μm)	1100 $^{\circ}\text{C}$	60 min	2 MPa	[169]

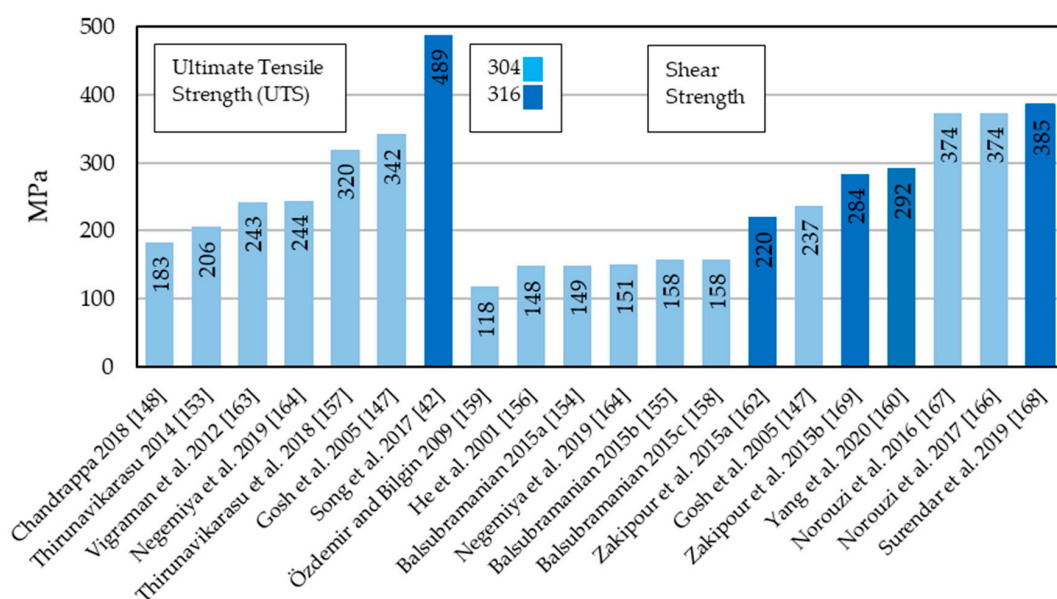


Figure 4. Reported ultimate tensile strength (UTS) (MPa) and shear strength (MPa) of 304 stainless steel and Ti-6Al-4V diffusion bonds and TLP bonds.

3.5. Diffusion Bonding and TLP Bonding of 304 and 316 to Cu and CuZrCr

Table 7 presents diffusion bonding and TLP bonding parameters of 304 stainless steel with Cu and CuZrCr that may be particularly relevant for parts in nuclear fusion applications. Akbar et al. [170] and Yilmaz [171] both present very systematic solid-state diffusion bonding studies of 304 stainless steel with copper. Optimized parameters reported by Yilmaz reach bond strength equivalent to the Cu base material receiving the same heat treatment, determined using both shear testing (bond strength 112 MPa vs. 113 MPa shear strength of the Cu base material) and tensile testing (bond strength 247 MPa

vs. 248 MPa UTS of the Cu base material). Studies from Kaya et al. [172] and Yuan et al. [50] use special diffusion bonding techniques that are interesting to elaborate on. In their study, Kaya et al. [172] use solid state diffusion bonding with and without an applied electric current to join 304 stainless steel to Cu. The obtained results using tensile testing, micro-hardness analysis as well as SEM (Scanning Electron Microscope) and EDS (Energy-Dispersive X-ray Spectroscopy) vary only slightly from one another in favor of the novel approach with electric current. Yuan et al. [50] use impulse pressure diffusion bonding (IPDB) that was briefly introduced earlier. Varying the pressure during the diffusion bonding process at a frequency of 0.5 Hz and using a 12.5 μm Ni-interlayer, samples reach 217 MPa UTS or 91% of the Cu-base material. This in itself is not too impressive given the data from Yilmaz [171] discussed earlier. Besides, Xiong et al. [173] reached UTS of 228 MPa using TLP bonding (without pressure variation) with a 100 μm thick Tin-Bronze (Alloy QSn 6.5–0.1: wt% 6–7 Sn, ≤ 0.3 Zn, 0.1–0.25 P, ≤ 0.05 Fe, ≤ 0.02 Pb, ≤ 0.002 Al, balance Cu) and a 5 μm Au interlayer. Yuan et al. [50] further used a Gleeble 1500 thermo-mechanical material testing system. These systems heat samples by applying a high electric voltage directly between the two ends of the specimens [174–177]. In this way, Yuan et al. realized heating rates of 5 $^{\circ}\text{C}/\text{s}$ that are much higher than those of classic diffusion bonding or TLP bonding (max. 10 $^{\circ}\text{C}/\text{min}$) where samples (often plate-shaped) are heated (ideally uniformly to avoid internal stress) through radiation from induction heating elements in the vacuum furnace. IPDB is nonetheless very promising as it may reduce costs for expensive interlayer materials or coating procedures during bonding. IPDB may further reduce the overall diffusion bonding time which is again beneficial.

Table 7. Reported parameters for diffusion bonding and TLP bonding of 304 and 316 to Cu and CuCrZr.

M1	M2	Interlayer	Temperature	Time	Pressure	Ref.
304	Cu	-	650 $^{\circ}\text{C}$	45 min	30.0 MPa	[170]
316L	Cu ¹	-	660 $^{\circ}\text{C}$	90 min	20.0 MPa	[178]
316L	Cu ¹	-	690 $^{\circ}\text{C}$	90 min	20.0 MPa	[178]
304	Cu	-	825 $^{\circ}\text{C}$	18 min	5.0 MPa	[171]
304L	Cu	Ni (12.5 μm)	850 $^{\circ}\text{C}$	20 min	5–20.0 MPa ²	[50]
304L	Cu	Sn Bronze-Au (100; 5 μm)	850 $^{\circ}\text{C}$	60 min	3.0 MPa	[173]
316	Cu ³	Au (20 μm)	850 $^{\circ}\text{C}$	60 min	4.8 MPa	[179]
304	Cu	Ni (10–15 μm)	850 $^{\circ}\text{C}$	60 min	8.0 MPa	[180]
316	CuCrZr	-	850 $^{\circ}\text{C}$	60 min	10.0 MPa	[181]
316	Cu ³	Au (20 μm)	850 $^{\circ}\text{C}$	60 min	NR	[182]
316	Cu ³	Au (20 μm)	850 $^{\circ}\text{C}$	120 min	9.8 MPa	[183]
304	Cu	-	875 $^{\circ}\text{C}$	30 min	3.0 MPa	[172]
316L	CuCrZr	Ni (25 μm)	900 $^{\circ}\text{C}$	15 min	5.0 MPa	[184] ⁴
316L	CuCrZr	-	900 $^{\circ}\text{C}$	15 min	7.0 MPa	[184] ⁴
316	Cu ³	-	900 $^{\circ}\text{C}$	60 min	4.8 MPa	[185]
304	Cu	-	900 $^{\circ}\text{C}$	60 min	10.0 MPa	[180]

¹ Oxygen-free high thermal conductivity (OFHC) copper, ² Impulse pressure diffusion bonding (IPDB), ³ Dispersion strengthened (DS) copper, ⁴ done with Gleeble using current through sample.

3.6. Diffusion Bonding and TLP Bonding of 304 and 316 to Zircaloy and Zr-Sn-Nb

Zircaloy and other zirconium alloys such as Zr-Sn-Nb are widely used in the nuclear industry due to their favorable neutron cross sections, adequate mechanical properties and excellent corrosion resistance [186,187]. Table 8 lists reported dissimilar diffusion bonding and TLP bonding studies of 304 and 316 stainless steel to Zircaloy and Zr-Sn-Nb. Zircaloy-2 and Zircaloy-4 have a melting point of 1850 $^{\circ}\text{C}$ [188], that is higher than the melting points of copper (1085 $^{\circ}\text{C}$) and titanium (1668 $^{\circ}\text{C}$). Dissimilar diffusion bonding and TLP bonding of 304 and 316 to Zircaloy and Zr-Sn-Nb was subsequently (in most cases) conducted at higher temperatures than dissimilar bonding of stainless steel to copper and titanium. Only three studies reported mechanical bond properties, so a quantitative comparison between the studies is challenging. Bhanumurthy et al. [189] joined 304L stainless steel to Zircaloy-2 using sandwiched Ni-Cu-Nb interlayers of 30–70 μm thickness each. The accomplished

bonds reached UTS of up to 450 MPa, and average UTS of roughly 400 MPa. Pan et al. [190] and Srikanth et al. [191] both joined 304L stainless steel to Zircaloy-4 reporting accomplished shear strengths of 166 MPa and 209 MPa, respectively.

Table 8. Reported parameters for diffusion bonding and TLP bonding of 304 and 316 to Zircaloy and Zr-Sn-Nb.

M1	M2	Interlayer	Temperature	Time	Pressure	Ref.
304L	Zircaloy-4	Ti-Ag (50; 50 μm)	800 °C	90 min	12.0 MPa	[190]
304L	Zircaloy-4	-	820 °C	45 min	7.5 MPa	[192]
304L	Zircaloy-4	-	850 °C	45 min	11.2 MPa	[193–197]
304L	Zircaloy-4	Ni-Ti (20;40 μm)	850 °C	60 min	20.0 MPa	[191]
304L	Zircaloy-2	Ni-Cu-Nb (30-70 μm)	870 °C	120 min	10.0 MPa	[189]
316L	Zircaloy-4	Fe-Ti (NR)	927 °C	15 min	NR	[84]
304L	Zircaloy-4	Cu (50 μm)	950 °C	45 min	2.0 MPa	[198]
304L	Zircaloy-4	-	950 °C	45 min	2.0 MPa	[193–197]
304L	Zircaloy-4	-	950 °C	45 min	2.2 MPa	[192]
304	Zr-Sn-Nb	Ni (5 μm)	1000 °C	30 min	NR	[199]
304L	Zircaloy-2	-	1000 °C	60 min	0.2 MPa	[200]
316L	Zircaloy-4	Ti (NR)	1000 °C	240 min	NR	[57,58]
304L	Zircaloy-4	-	1020 °C	45 min	0.8 MPa	[193–197]
304L	Zircaloy-4	-	1050 °C	45 min	0.2 MPa	[193–197]
316L	Zircaloy-4	Ti (NR)	1050 °C	60 min	NR	[57,58]
304L	Zircaloy-2	-	1100 °C	60 min	0.3 MPa	[200]
304L	Zircaloy-4	Ta (NR)	1150 °C	180 min	NR	[201]

3.7. Diffusion Bonding and TLP Bonding of 304 and 316 to Other Materials

Table 9 provides an overview of reported diffusion bonding and TLP bonding experiments of 304 and 316 stainless steels to other materials not discussed in the previous chapters. Magnesium alloys (AM60 and AZ31), mild steel (EN3B), low alloy steel (A533B), Nickel, titanium alloy 6246, stainless steels, cast iron and Kovar were bonded with 304 and 316 stainless steel. In addition, a number of ceramic materials (Al_2O_3 , Ni_3Al , Si_3N_4 , Sialon, TiC, WC and ZrO_2) were bonded to 304 and 316 stainless steel using diffusion bonding or TLP bonding. The large differences in the coefficient of the thermal expansion of steel and ceramics make joining challenging and is the reason that interlayers are often used [202,203].

Table 9. Reported parameters for diffusion bonding and TLP bonding of 304 and 316 to various other materials not discussed previously.

M1	M2	Interlayer	Temperature	Time	Pressure	Ref.
304	AM60	Zn (1 μm)	470 °C	30 min	NR	[204]
316L	AZ 31	Cu (20 μm)	530 °C	60 min	<1 MPa	[205]
316L	AZ 31	Ni (20 μm)	510 °C	60 min	<1 MPa	[205]
316L	AZ 31	Ni (20 μm)	510 °C	20 min	<1 MPa	[206,207]
316L	AZ 31	Cu (20 μm)	530 °C	30 min	<1 MPa	[207]
316	A533B	Ni (NR)	900 °C	120 min	95 MPa	[208]
316	A533B	-	1050 °C	150 min	95 MPa	[208]
316	En3B	Ni (NR)	900 °C	120 min	95 MPa	[208]
316	En3B	-	1050 °C	150 min	95 MPa	[208]
304	Ni	Ni (10–15 μm)	800 °C	60 min	10 MPa	[209]
316L	Ti 6242	-	900 °C	15 min	15 MPa	[131]
316L	Ti 6242	-	900 °C	15 min	15 MPa	[210]
304	SAF 2507	BNi-2 (50 μm)	1045 °C	45 min	NR	[211]

Table 9. Cont.

M1	M2	Interlayer	Temperature	Time	Pressure	Ref.
316	355	-	1050 °C	60 min	13 MPa	[212]
316L	Cast Iron	-	1000 °C	30 min	10 MPa	[213]
316L	Kovar	Ni (70 µm)	900 °C	240 min	35 MPa	[214]
316L	Kovar	Co (50 µm)	945 °C	150 min	10 MPa	[215]
304	Al ₂ O ₃	Ti (500 µm)	800 °C	15 min	15 MPa	[216]
304	Al ₂ O ₃	Ti (500 µm)	900 °C	60 min	15 MPa	[217]
316L	Ni ₃ Al	Ni (10 µm)	1000 °C	240 min	5 MPa	[218]
316L	Ni ₃ Al	-	1050 °C	30 min	6 MPa	[219]
316	Si ₃ N ₄	Invar (250 µm)	1000 °C	90 min	7 MPa	[220]
316	Si ₃ N ₄	-	1100 °C	120 min	4–5 MPa	[221]
316L	Sialon	-	1200 °C	60 min	15 MPa	[222]
316L	Sialon	-	1250 °C	60 min	15 MPa	[223]
304	TiC	Ti-Nb-Cu (400 µm)	925 °C	20 min	8 MPa	[224]
316	WC	Ni (NR)	1200 °C	30 min	1 MPa	[225]
316	ZrO ₂	Ni (300 µm)	900 °C	90 min	20 MPa	[226]
316	ZrO ₂	-	1200 °C	60 min	10 MPa	[227]

3.8. Hot Isostatic Pressing (HIP) of 304 and 316 (Similar and Dissimilar Joints)

HIP was invented in 1955 for diffusion bonding applications in the nuclear industry [228]. Besides interfacial bonding, it finds much wider application now in upgrading castings, densifying pre-sintered components, consolidating powders [229,230] and post-treating parts produced by selective laser melting (SLM). HIP can also be used to eliminate voids at diffusion bonded interfaces [108]. HIP is often used for diffusion bonding of first-wall structures in fusion reactors. Most notably CuCrZr [231] and dispersion strengthened copper (DS Cu) [232] are bonded. Studies examining HIP of similar and dissimilar joints of 304 and 316 stainless steel are listed in Table 10.

Table 10. Reported parameters for hot isostatic pressing (HIP) of 304 and 316 (similar and dissimilar joints).

M1	M2	Interlayer	Temperature	Time	Pressure	Ref.
316L	CuCrZr	Ni (6 µm)	900 °C	120 min	130 MPa	[233]
316LN	CuCrZr	Fe ₄₂ Ni (NR)	920 °C	180 min	120 MPa	[27]
316LN	CuCrZr	-	980 °C	120 min	140 MPa	[234]
316L	CuCrZr	Ni (6 µm)	980 °C	120 min	140 MPa	[235]
316LN	CuCrZr	Ni (NR)	1000 °C	60 min	130 MPa	[27]
316L	CuCrZr	-	1040 °C	120 min	103 MPa	[236]
316LN	CuCrZr	-	1040 °C	120 min	140 MPa	[234,237]
316L	DS Cu	-	1050 °C	120 min	150 MPa	[238–241]
316LN	DS Cu	-	1090 °C	120 min	100 MPa	[242]
316LN	DS Cu	Ni (NR)	1090 °C	120 min	100 MPa	[242]
316LN	DS Cu	-	1125 °C	240 min	100 MPa	[243]
316	W	Ti (100 µm)	930 °C	120 min	100 MPa	[244]
316L	W	Cu (250 µm)	1050 °C	120 min	150 MPa	[245]
304	304	-	1100 °C	150 min	100 MPa	[108]
316LN	316LN	-	1100 °C	120 min	150 MPa	[246]

4. Conclusions

This work provides an overview of similar and dissimilar diffusion bonding and TLP bonding of 304 and 316 stainless steel by reporting on the main process parameters: bonding temperature, bonding time and bonding pressure as well as used interlayer(s), if any. Diffusion bonding and TLP bonding are commercially used processes and it is noteworthy that reported parameters for identical material combinations can vary considerably from one another. To compare different studies, we put much emphasis on quantitatively reported results such as tensile- and shear strength rather than qualitative

results that are much more difficult to compare. This may overemphasize the importance of mechanical testing versus qualitative testing. We are also aware that this is in many cases an apple and orange comparison, since pre-and post-treatments are not taken into consideration and additional processing parameters, such as the sample geometry, can influence the bond quality. Nevertheless, both apples and oranges have features in common so that there may be something to learn from these comparisons. Most importantly we want to use this review to provide an overview of the conducted experiments on the market to assist upcoming diffusion bonding and TLP bonding studies of 304 and 316 stainless steel.

We believe that future studies on diffusion bonding and TLP bonding should aim to report quantitative results such as tensile- and shear strength so that the overall bond quality can be quickly assessed. We also urge researchers to report the experimental set-up used to generate this data, and ask them to follow standardized testing whenever possible. Since the strength of seemingly similar materials also showed considerable differences in the reported data, we further urge researchers to conduct similar experiments with the base material(s) used. The quality of the generated diffusion bonds can also show significant differences and we recommend a minimum of three samples for each data point. We are aware that diffusion bonding apparatuses often do not allow the production of samples suitable for tensile testing since a minimum height needs to be realized. Finding reliable correlations that allow a comparison between tensile- and shear-tested diffusion bonded and TLP bonded samples was identified as a promising field of research.

Similar and dissimilar diffusion bonding and TLP bonding of 304 and 316 stainless steel is already used commercially and future experiments should aim to further optimize existing bonding parameters. Technical parameters (temperature, time, pressure, interlayers, etc.) should be optimized to accomplish the same or better bond qualities with fewer resources, resulting in more economically and ecologically sound processes. Here, particularly the reduction of expensive interlayers and complicated surface treatments should be omitted as far as possible. In this regard creative techniques such as applied temperature gradients as proposed by Shirzadi and impulse pressure diffusion bonding (IPDB) are promising fields of future diffusion bonding and TLP bonding research.

Funding: This research received no external funding.

Acknowledgments: The authors are grateful to the Deanship of Scientific Research, King Saud University for funding through Vice Deanship of Scientific Research Chairs.

Conflicts of Interest: The authors declare no conflict of interest.

References

1. Kazakov, N.F. *Diffusion Bonding of Materials*; Elsevier: Oxford, UK, 1985; ISBN 978-1483118130.
2. Carlone, P.; Astarita, A. Dissimilar Metal Welding. *Metals* **2019**, *9*, 1206. [[CrossRef](#)]
3. Kah, P.; Shrestha, M.; Martikainen, J. Trends in Joining Dissimilar Metals by Welding. *Appl. Mech. Mater.* **2014**, *440*, 269–276. [[CrossRef](#)]
4. Song, G.; Li, T.; Yu, J.; Liu, L. A Review of Bonding Immiscible Mg/Steel. *Materials* **2018**, *11*, 2515. [[CrossRef](#)] [[PubMed](#)]
5. Gietzelt, T.; Toth, V.; Huell, A. Challenges of Diffusion Bonding of Different Classes of Stainless Steels. *Adv. Eng. Mater.* **2017**, *20*, 1700367. [[CrossRef](#)]
6. Gietzelt, T.; Toth, V.; Huell, A.; Dittmeyer, R. Determining the Dependence of Deformation during Diffusion Welding on the Aspect Ratio Using Samples Made of SS 304 (1.4301). *Adv. Eng. Mater.* **2017**, *19*, 1–8. [[CrossRef](#)]
7. Cook, G.O.; Sorensen, C.D. Overview of transient liquid phase and partial transient liquid phase bonding. *J. Mater. Sci.* **2011**, *46*, 5305–5323. [[CrossRef](#)]
8. Gale, W.; Butts, D. Transient liquid phase bonding. *Sci. Technol. Weld. Join.* **2004**, *9*, 283–300. [[CrossRef](#)]
9. Shirzadi, A.A.; Assadi, H.; Wallach, E.R. Interface evolution and bond strength when diffusion bonding materials with stable oxide films. *Surf. Interface Anal.* **2001**, *31*, 609–618. [[CrossRef](#)]
10. MacDonald, W.; Eagar, T. Transient liquid phase bonding. *Annu. Rev. Mater. Sci.* **1992**, *22*, 23–46. [[CrossRef](#)]
11. Was, G.S.; Ukai, S. *Austenitic Stainless Steels*; Elsevier Inc: Amsterdam, The Netherlands, 2019; ISBN 978-0-12-397046-6.

12. Michler, T. Austenitic Stainless Steels. *Ref. Modul. Mater. Sci. Mater. Eng.* **2016**, 1–6. [[CrossRef](#)]
13. Cobb, H.M. *The History of Stainless Steel*; ASM International: Cleveland, OH, USA, 2010; ISBN 9781615030118.
14. McGuire, M.F. *Stainless Steels for Design Engineers*; ASM International: Cleveland, OH, USA, 2008; ISBN 978-0-87170-717-8.
15. Campbell, F. *Manufacturing Technology for Aerospace Structural Materials*; Elsevier: Amsterdam, The Netherlands, 2006.
16. Lee, H.; Yoon, J.; Yoo, J. Manufacturing of Aerospace Parts with Diffusion Bonding Technology. *Appl. Mech. Mater.* **2011**, *87*, 182–185. [[CrossRef](#)]
17. Simões, S. Diffusion Bonding and Brazing of Advanced Materials. *Metals* **2018**, *8*, 959. [[CrossRef](#)]
18. Shin, J.; Yoon, S.H. Thermal and hydraulic performance of a printed circuit heat exchanger using two-phase nitrogen. *Appl. Therm. Eng.* **2020**, *168*, 114802. [[CrossRef](#)]
19. Li, Q.; Flamant, G.; Yuan, X.; Neveu, P.; Luo, L. Compact heat exchangers: A review and future applications for a new generation of high temperature solar receivers. *Renew. Sustain. Energy Rev.* **2011**, *15*, 4855–4875. [[CrossRef](#)]
20. Pra, F.; Tochon, P.; Mauget, C.; Fokkens, J.; Willemsen, S. Promising designs of compact heat exchangers for modular HTRs using the Brayton cycle. *Nucl. Eng. Des.* **2008**, *238*, 3160–3173. [[CrossRef](#)]
21. Wilden, J.; Jahn, S.; Beck, W. Some examples of current diffusion bonding applications. *Mater. Sci. Eng. Technol.* **2008**, *39*, 349–352. [[CrossRef](#)]
22. Mylavarapu, S.K.; Sun, X.; Christensen, R.N.; Unocic, R.R.; Glosup, R.E.; Patterson, M.W. Fabrication and design aspects of high-temperature compact diffusion bonded heat exchangers. *Nucl. Eng. Des.* **2012**, *249*, 49–56. [[CrossRef](#)]
23. Chai, L.; Tassou, S.A. A review of printed circuit heat exchangers for helium and supercritical CO₂ Brayton cycles. *Therm. Sci. Eng. Prog.* **2020**, *18*, 100543. [[CrossRef](#)]
24. Brandner, J.J.; Anurjew, E.; Bohn, L.; Hansjosten, E.; Henning, T.; Schygulla, U.; Wenka, A.; Schubert, K. Concepts and realization of microstructure heat exchangers for enhanced heat transfer. *Exp. Therm. Fluid Sci.* **2006**, *30*, 801–809. [[CrossRef](#)]
25. Sabharwall, P.; Clark, D.; Glazoff, M.; Zheng, G.; Sridharan, K.; Anderson, M. Advanced heat exchanger development for molten salts. *Nucl. Eng. Des.* **2014**, *280*, 42–56. [[CrossRef](#)]
26. Rowcliff, A.; Zinkle, S.; Stubbins, J.; Edwards, D.; Alexander, D. Austenitic stainless steels and high strength copper alloys for fusion components. *J. Nucl. Mater.* **2008**, *263*, 183–192. [[CrossRef](#)]
27. Ivanov, A.D.; Sato, S.; Marois, G. Le Evaluation of hot isostatic pressing for joining of fusion reactor structural components. *J. Nucl. Mater.* **2000**, *287*, 35–42. [[CrossRef](#)]
28. Suri, A.; Krishnamurthy, N.; Batra, I. Materials issues in fusion reactors. *J. Phys. Conf. Ser.* **2010**, *208*, 012001. [[CrossRef](#)]
29. Montemor, M.; Ferreira, M.; Hakiki, N.; Da Cunha Belo, M. Chemical composition and electronic structure of the oxide films formed on 316L stainless steel and nickel based alloys in high temperature aqueous environments. *Corros. Sci.* **2000**, *42*, 1635–1650. [[CrossRef](#)]
30. Fang, Y.; Jiang, X.; Mo, D.; Zhu, D.; Luo, Z. A review on dissimilar metals' welding methods and mechanisms with interlayer. *Int. J. Adv. Manuf. Technol.* **2019**, *102*, 2845–2863. [[CrossRef](#)]
31. Cai, W.; Daehn, G.; Vivek, A.; Li, J.; Khan, H.; Mishra, R.; Komarasamy, M. A state-of-the-art review on solid-state metal joining. *J. Manuf. Sci. Eng.* **2018**, *141*, 031012. [[CrossRef](#)]
32. Tomashchuk, I.; Sallamand, P. Metallurgical Strategies for the Joining of Titanium Alloys with Steels. *Adv. Eng. Mater.* **2018**, *20*, 1700764. [[CrossRef](#)]
33. Mo, D.; Song, T.; Fang, Y.; Jiang, X.; Luo, C.Q.; Simpson, M.D.; Luo, Z. A Review on Diffusion Bonding between Titanium Alloys and Stainless Steels. *Adv. Mater. Sci. Eng.* **2018**. [[CrossRef](#)]
34. Gietzelt, T.; Toth, V.; Huell, A.; Messerschmidt, F.; Dittmeyer, R. Systematic investigation of the diffusion welding behavior of the austenitic stainless steel 304 (1.4301). *Adv. Eng. Mater.* **2014**, *16*, 1381–1390. [[CrossRef](#)]
35. Lee, M.K.; Lee, J.G.; Choi, Y.H.; Kim, D.W.; Rhee, C.K.; Lee, Y.B.; Hong, S.J. Interlayer engineering for dissimilar bonding of titanium to stainless steel. *Mater. Lett.* **2010**, *64*, 1105–1108. [[CrossRef](#)]
36. Moravec, J.; Novakova, I.; Kik, T. Possibilities of using interlayers during diffusion welding of Ti Gr₂ and AISI 316L. *MATEC Web Conf.* **2018**, *244*, 1–8. [[CrossRef](#)]
37. Shirzadi, A.A.; Zhu, Y.; Bhadeshia, H.K.D.H. Joining ceramics to metals using metallic foam. *Mater. Sci. Eng. A* **2008**, *496*, 501–506. [[CrossRef](#)]

38. Özdemir, N.; Aksoy, M.; Orhan, N. Effect of graphite shape in vacuum-free diffusion bonding of nodular cast iron with gray cast iron. *J. Mater. Process. Technol.* **2003**, *141*, 228–233. [[CrossRef](#)]
39. Kato, H.; Shibata, M.; Yoshikawa, K. Diffusion welding of Ti/Ti and Ti/stainless steel rods under phase transformation in air. *Mater. Sci. Technol.* **1986**, *2*, 405–409. [[CrossRef](#)]
40. Calderon, P.; Walmsley, D.; Munir, Z. An Investigation of Diffusion Welding of Pure and Alloyed Aluminum to Type 316 Stainless Steel. *Weld. J.* **1985**, *64*, 104–114.
41. Cox, M.J.; Kim, M.J.; Carpenter, R.W. Interface Nanochemistry Effects on Stainless Steel Diffusion Bonding. *Metall. Mater. Trans. A* **2002**, *33*, 437–442. [[CrossRef](#)]
42. Song, T.F.; Jiang, X.S.; Shao, Z.Y.; Fang, Y.J.; Mo, D.F.; Zhu, D.G.; Zhu, M.H. Microstructure and mechanical properties of vacuum diffusion bonded joints between Ti-6Al-4V titanium alloy and AISI316L stainless steel using Cu/Nb multi-interlayer. *Vacuum* **2017**, *145*, 68–76. [[CrossRef](#)]
43. Shirzadi, A.A.; Wallach, E.R. Analytical Modeling of transient liquid phase (TLP) diffusion bonding when a temperature gradient is imposed. *Acta Metall.* **1999**, *47*, 3551–3560.
44. Shirzadi, A.A.; Wallach, E.R. Metal Bonding. US Patent 6,257,481 B1, 10 July 2001.
45. Shirzadi, A.A.; Wallach, E.R. Temperature gradient transient liquid phase diffusion bonding: A new method for joining advanced materials. *Sci. Technol. Weld. Join.* **1997**, *2*, 89–94. [[CrossRef](#)]
46. Sheng, G.M. An experimental investigation of phase transformation superplastic diffusion bonding of titanium alloy to stainless steel. *J. Mater. Sci.* **2005**, *40*, 6385–6390. [[CrossRef](#)]
47. Sharma, G.; Tiwari, L.; Kumar, D. Impulse Pressure Assisted Diffusion Bonding of Low Carbon Steel Using Silver Interlayer. *Trans. Indian Inst. Met.* **2018**, *71*, 11–21. [[CrossRef](#)]
48. Sharma, G.; Dwivedi, D.K. Impulse pressure-assisted diffusion bonding of ferritic stainless steel. *Int. J. Adv. Manuf. Technol.* **2018**, *95*, 4293–4305. [[CrossRef](#)]
49. Wang, F.; Sheng, G.; Deng, Y.-Q. Impulse pressuring diffusion bonding of titanium to 304 stainless steel using pure Ni interlayer. *Rare Met.* **2014**, *35*, 331–336. [[CrossRef](#)]
50. Yuan, X.; Tang, K.; Deng, Y.; Luo, J.; Sheng, G. Impulse pressuring diffusion bonding of a copper alloy to a stainless steel with/without a pure nickel interlayer. *Mater. Des.* **2013**, *52*, 359–366. [[CrossRef](#)]
51. Yuan, X.J.; Sheng, G.M.; Qin, B.; Huang, W.Z.; Zhou, B. Impulse pressuring diffusion bonding of titanium alloy to stainless steel. *Mater. Charact.* **2008**, *59*, 930–936. [[CrossRef](#)]
52. Han, J.; Sheng, G.M.; Zhou, X.L.; Sun, J.X. Pulse Pressuring Diffusion Bonding of Ti Alloy/Austenite Stainless Steel Processed by Surface Self-nanocrystallization. *ISIJ Int.* **2009**, *49*, 86–91. [[CrossRef](#)]
53. Huang, L.; Sheng, G.; Li, J.; Huang, G.; Yuan, X. Partial transient-liquid-phase bonding of TiC cermet to stainless steel using impulse pressuring with Ti/Cu/Nb interlayer. *J. Cent. South Univ.* **2018**, *25*, 1025–1032. [[CrossRef](#)]
54. Jia, L.; Guangmin, S. Diffusion Bonding of TiC Cermet to Stainless Steel Using Impulse Pressuring with Ti-Nb Interlayer. *Rare Met. Mater. Eng.* **2017**, *46*, 882–887. [[CrossRef](#)]
55. Yuan, X.; Sheng, G.; Tang, K. Effect of interlayer type on microstructure and mechanical property of impulse pressuring diffusion bonded joints in austenitic stainless steel to α titanium alloy. *Mater. Res. Innov.* **2013**, *17*, 186–189. [[CrossRef](#)]
56. Yuan, X.; Sheng, G.; Luo, J.; Li, J. Microstructural characteristics of joint region during diffusion-brazing of magnesium alloy and stainless steel using pure copper interlayer. *Trans. Nonferrous Met. Soc. China* **2013**, *23*, 599–604. [[CrossRef](#)]
57. Akhter, J.I.; Ahmad, M.; Iqbal, M.; Akhtar, M.; Shaikh, M.A. Formation of dendritic structure in the diffusion zone of the bonded Zircaloy-4 and stainless steel 316L in the presence of Ti interlayer. *J. Alloys Compd.* **2005**, *399*, 96–100. [[CrossRef](#)]
58. Akhter, J.I.; Ahmad, M.; Ali, G. Diffusion bonding of Ti coated Zircaloy-4 and 316-L stainless steel. *Mater. Charact.* **2009**, *60*, 193–196. [[CrossRef](#)]
59. Munis, A.; Zheng, M.; Akhter, J.; Ahmad, M. Characterization of Bonded Zone and Evaluation of Cracking in Vacuum Brazed Zircaloy-4 and Stainless Steel 316L Joint. *Arch. Met. Mater.* **2019**, *64*, 707–713.
60. Mukherjee, A.B.; Laik, A.; Kain, V.; Chakravartty, J.K. Shrinkage-Stress Assisted Diffusion Bonds Between Titanium and Stainless Steel: A Novel Technique. *J. Mater. Eng. Perform.* **2016**, *25*, 4425–4436. [[CrossRef](#)]
61. Kang, S.; Chen, Y.; Liu, H. Brazing diffusion bonding of micro-nickel cylinders and SUS-316 stainless steel. *J. Mater. Process. Technol.* **2005**, *168*, 286–290. [[CrossRef](#)]

62. Kale, G.B.; Patil, R.V.; Gawade, P.S. Interdiffusion studies in titanium-304 stainless steel system. *J. Nucl. Mater.* **1998**, *257*, 44–50. [\[CrossRef\]](#)
63. Salmaliyan, M.; Shamanian, M. Formation mechanism of intermetallic components during dissimilar diffusion bonding of IN718/BNi-2/AISI 316L by TLP process. *Heat Mass Transf.* **2019**, *55*, 2083–2093. [\[CrossRef\]](#)
64. Ganesan, V.; Seetharaman, V.; Raghunathan, V.S. Interdiffusion in the type 316 austenitic stainless steel/iron. *J. Nucl. Mater.* **1983**, *118*, 313–319. [\[CrossRef\]](#)
65. Deqing, W.; Ziyuan, S.; Ruobin, Q. Cladding of stainless steel on aluminum and carbon steel by interlayer diffusion bonding. *Scr. Mater.* **2007**, *56*, 369–372. [\[CrossRef\]](#)
66. Harumoto, T.; Ohashi, O.; Tsushima, H.; Narui, M.; Aihara, K.; Ishiguro, T. Thermal Stress-Based Diffusion Bonding Method: The Case of Oxygen Free Copper to 316L Stainless Steel. *Mater. Trans.* **2015**, *56*, 1683–1687. [\[CrossRef\]](#)
67. Ghaderi, S.; Karimzadeh, F.; Ashra, A. Evaluation of microstructure and mechanical properties of transient liquid phase bonding of Inconel 718 and nano/ultrafine-grained 304L stainless steel. *J. Manuf. Process.* **2020**, *49*, 162–174. [\[CrossRef\]](#)
68. Reuven, R.; Bolind, A.; Haneklaus, N.; Andreades, C.; Cionea, C.; Buster, G.; Hosemann, P.; Peterson, P. Ni Interlayer to Improve Low-Pressure Diffusion Bonding of 316L SS Press Fit Tube-to-Tubesheet Joints for Coiled Tube Gas Heaters. *J. Nucl. Eng. Radiat. Sci.* **2017**, *3*, 1–6. [\[CrossRef\]](#)
69. Haneklaus, N.; Reuven, R.; Cionea, C.; Hosemann, P.; Peterson, P.F. Tube expansion and diffusion bonding of 316L stainless steel tube-to-tube sheet joints using a commercial roller tube expander. *J. Mater. Process. Tech.* **2016**, *234*, 27–32. [\[CrossRef\]](#)
70. Haneklaus, N.; Reuven, R.; Cionea, C.; Hosemann, P.; Peterson, P.F. Development of engineering parameters for low pressure diffusion bonds of 316 SS tube-to-tube sheet joints for fhr heat exchangers. In *TMS 2016 145th Annual Meeting & Exhibition*; Springer: Cham, Switzerland, 2016; pp. 583–588.
71. Shiue, R.; Chen, C.; Wu, S. Memory Alloy and 316L Stainless Steel with Two Sliver-Based Fillers. *Metall. Mater. Trans. A* **2015**, *46*, 2364–2371. [\[CrossRef\]](#)
72. Dong, H.; Yang, Z.; Wang, Z.; Deng, D.; Dong, C. Vacuum Brazing TC4 Titanium Alloy to 304 Stainless Steel with Cu-Ti-Ni-Zr-V Amorphous Alloy Foil. *J. Mater. Eng. Perform.* **2014**, *23*, 3770–3777. [\[CrossRef\]](#)
73. Shafiei, A.; Abachi, P.; Dehghani, K.; Pourazarang, K. On the Formation of Intermetallics during the Furnace Brazing of Pure Titanium to 304 Stainless Steel Using Ag (30–50%)–Cu Filler Metals. *Mater. Manuf. Process.* **2010**, *25*, 37–41. [\[CrossRef\]](#)
74. Hdz-Garcia, H.; Martinez, A.; Munoz-Arroyo, R.; Acevedo-Davila, J.; Garcia-Vazquez, F.; Reyes-Valdes, F. Effects of Silicon Nanoparticles on the Transient Liquid Phase Bonding of 304 Stainless Steel. *J. Mater. Sci. Technol.* **2014**, *30*, 259–262. [\[CrossRef\]](#)
75. Eluri, R.; Paul, B. Hermetic joining of 316L stainless steel using a patterned nickel nanoparticle interlayer. *J. Manuf. Process.* **2012**, *14*, 471–477. [\[CrossRef\]](#)
76. Chung, T.; Kim, J.; Bang, J.; Rhee, B.; Nam, D. Microstructures of brazing zone between titanium alloy and stainless steel using various filler metals. *Trans. Nonferrous Met. Soc. China* **2012**, *22*, S639–S644. [\[CrossRef\]](#)
77. Abed, A.; Jalham, I.S.; Hendry, A. Wetting and reaction between sialon, stainless steel and Cu-Ag brazing alloys containing Ti. *J. Eur. Ceram. Soc.* **2001**, *21*, 283–290. [\[CrossRef\]](#)
78. González-Sánchez, J.; Verduzco, J.; Lemus-Ruiz, J.; Téllez, M.; Torres, A.; Torres, R. Corrosion resistance of stainless steel joints bonded with a Ni-based amorphous interlayer. *Anti Corros. Methods Mater.* **2007**, *54*, 68–73. [\[CrossRef\]](#)
79. Verduzco, J.A.; González-sánchez, J.; Verduzco, V.H.; Solís, J.; Lemus-ruiz, J. Journal of Materials Processing Technology Microstructure and electrochemical properties of the bonding zone of AISI 316L steel joined with a Fe-based amorphous foil. *J. Mater. Process. Technol.* **2010**, *210*, 1051–1060. [\[CrossRef\]](#)
80. Tashi, R.S.; Mousavi, S.A.A.A.; Atabaki, M.M. Diffusion brazing of Ti–6Al–4V and austenitic stainless steel using silver-based interlayer. *Mater. Des.* **2014**, *54*, 161–167. [\[CrossRef\]](#)
81. Bajgholi, M.E.; Tashi, R.S.; Mousavi, A.A.A.; Dehkordi, E.H. An Investigation on Metallurgical and Mechanical Properties of Vacuum Brazed Ti-6Al-4V to 316L Stainless Steel Using Zr-Based Filler Metal. *J. Adv. Mater. Process.* **2013**, *1*, 47–54.
82. Lee, S.; Kang, K.-H.; Hong, H.S.; Yun, Y. Microstructure and Interfacial Morphologies of Brazed NiO-YSZ/316 stainless steel using B-Ni2 brazing alloy. *Mater. Test. Join. Technol.* **2010**, *52*, 257–262. [\[CrossRef\]](#)

83. Paiva, O.C.; Barbosa, M.A. Microstructure, mechanical properties and chemical degradation of brazed AISI 316 stainless steel/alumina systems. *Mater. Sci. Eng. A* **2008**, *480*, 306–315. [[CrossRef](#)]
84. Kale, G.B.; Bhanumurthy, K.; Ratnakala, K.C.; Khera, S.K. Solid State Bonding of Zircaloy-2 with Stainless Steel. *J. Nucl. Mater.* **1986**, *138*, 73–80. [[CrossRef](#)]
85. Lugscheider, E.; Partz, K.D.; Lison, R. Thermal and Metallurgical Influences on AISI 316 and Inconel 625 by High Temperature Brazing with Nickel Base Filler Metals. *Weld. Res. Suppl.* **1982**, *61*, 329–333.
86. Kumar, A.; Ganesh, P.; Kaul, R.; Bhatnagar, V.K.; Yedle, K.; Sankar, P.R.; Sindal, B.K.; Kumar, K.; Singh, M.K.; Rai, S.K.; et al. A New Vacuum Brazing Route for Niobium-316L Stainless Steel Transition Joints for Superconducting RF Cavities. *J. Mater. Eng. Perform.* **2015**, *24*, 952–963. [[CrossRef](#)]
87. Yue, X.; He, P.; Feng, J.C.; Zhang, J.H.; Zhu, F.Q. Microstructure and interfacial reactions of vacuum brazing titanium alloy to stainless steel using an AgCuTi filler metal. *Mater. Charact.* **2008**, *59*, 1721–1727. [[CrossRef](#)]
88. Xia, Y.; Dong, H.; Hao, X.; Li, P.; Li, S. Vacuum brazing of Ti6Al4V alloy to 316L stainless steel using a Ti-Cu-based amorphous filler metal. *J. Mater. Process. Tech.* **2019**, *269*, 35–44. [[CrossRef](#)]
89. Xia, Y.; Dong, H.; Zhang, R.; Wang, Y.; Hao, X.; Li, P.; Dong, C. Interfacial microstructure and shear strength of Ti6Al4V alloy/316 L stainless steel joint brazed with $Ti_{33.3}Zr_{16.7}Cu_{50-x}Ni_x$ amorphous filler metals. *Mater. Des.* **2020**, *187*, 108380. [[CrossRef](#)]
90. Xia, Y.; Li, P.; Hao, X.; Dong, H. Interfacial microstructure and mechanical property of TC4 titanium alloy/316L stainless steel joint brazed with Ti-Zr-Cu-Ni-V amorphous filler metal. *J. Manuf. Process.* **2018**, *35*, 382–395. [[CrossRef](#)]
91. Roos, A.; Winkler, M.; Wimmer, G.; Dos Santos, J.F.; Hanke, S. New Approach on Solid State Joining of Stainless Steel Tube to Tube Sheet Joints. In *ASME 2017 Pressure Vessels and Piping Conference*; American Society of Mechanical Engineers Digital Collection: New York, NY, USA, 2017; pp. 1–8.
92. Haneklaus, N.; Cionea, C.; Reuven, R.; Frazer, D.; Hosemann, P.; Peterson, P.F. Hybrid friction diffusion bonding of 316L stainless steel tube-to-tube sheet joints for coil-wound heat exchangers. *J. Mech. Sci. Technol.* **2016**, *30*, 4925–4930. [[CrossRef](#)]
93. Esmailzadeh, R.; Salimi, M.; Zamani, C.; Hadian, A.M.; Hadian, A. Effects of milling time and temperature on phase evolution of AISI 316 stainless steel powder and subsequent sintering. *J. Alloys Compd.* **2018**, *766*, 341–348. [[CrossRef](#)]
94. Safarian, A.; Suba, M.; Karata, Ç. The effect of sintering parameters on diffusion bonding of 316L stainless steel in inserted metal injection molding. *Int. J. Adv. Manuf. Technol.* **2016**, *89*, 2165–2173. [[CrossRef](#)]
95. Sahli, M.; Lebled, A.; Gelin, J.; Barrière, T.; Necib, B. Numerical simulation and experimental analysis of solid-state sintering response of 316 L stainless steel micro-parts manufactured by metal injection molding. *Int. J. Adv. Manuf. Technol.* **2015**, *79*, 2079–2092. [[CrossRef](#)]
96. Qin, L.; Hu, J.; Cui, C.; Wang, H.; Guo, Z. Reaction sintering and joining nickel aluminide to AISI 316 stainless steel by self-propagating high temperature synthesis. *Mater. Sci. Technol.* **2009**, *25*, 1364–1368. [[CrossRef](#)]
97. Gal, C.W.; Han, S.S.; Han, J.S.; Lin, D.; Park, S.J. Investigation on Stainless steel 316L/Zirconia Joint Part fabricated by Powder Injection Molding. *Appl. Ceram. Technol.* **2019**, *16*, 315–323. [[CrossRef](#)]
98. Hasan, M.; Zhao, J.; Huang, Z.; Chang, L.; Zhou, H.; Jiang, Z. Analysis of sintering and bonding of ultra fine WC powder and stainless steel by hot compaction diffusion bonding. *Fusion Eng. Des.* **2018**, *133*, 39–50. [[CrossRef](#)]
99. Verma, D.; Singh, J.; Varma, A.H.; Tomar, V. Evaluation of Incoherent Interface Strength of Solid-State-Bonded Ti64/Stainless Steel Under Dynamic Impact Loading. *JOM* **2015**, *67*, 1694–1703. [[CrossRef](#)]
100. Firouzdor, V.; Simchi, A.; Kokabi, A. An investigation of the densification and microstructural evolution of M2/316L stepwise graded composite during co-sintering. *J. Mater. Sci.* **2008**, *43*, 55–63. [[CrossRef](#)]
101. Park, D.Y.; Lee, S.W.; Park, S.J.; Kwon, Y. Effects of Particle Sizes on Sintering Behavior of 316L Stainless Steel Powder. *Metall. Mater. Trans. A* **2013**, *44*, 1508–1518. [[CrossRef](#)]
102. Jeon, B.; Sohn, S.H.O.; Lee, W.; Han, C.; Kim, Y.D.O.; Choi, H. Double step sintering behavior of 316L nanoparticle dispersed micro-sphere powder. *Arch. Metall. Mater.* **2015**, *60*, 11–14. [[CrossRef](#)]
103. Gawde, P.S.; Kishore, R.; Pappachan, A.L.; Kale, G.B.; Dey, G.K. Low temperature diffusion bonding of stainless steel. *Trans. Indian Inst. Met.* **2010**, *63*, 853–857. [[CrossRef](#)]
104. Lamjiri, R.J.; Ekrami, A. Transient Liquid Diffusion Bonding of AISI304 Stainless Steel with a Nickel Base Interlayer. *Defect Diffus. Forum* **2017**, *380*, 48–54. [[CrossRef](#)]

105. Kazazi, A.; Ekrami, A. Corrosion behavior of TLP bonded stainless steel 304 with Ni-based interlayer. *J. Manuf. Process.* **2019**, *42*, 131–138. [[CrossRef](#)]
106. Sadeghian, M.; Ekrami, A.; Jamshidi, R. Transient liquid phase bonding of 304 stainless steel using a Co-based interlayer. *Sci. Technol. Weld. Join.* **2017**, *22*, 666–672. [[CrossRef](#)]
107. Atabaki, M.; Wati, J.; Idris, J. Transient liquid phase diffusion bonding of stainless steel 304. *Met. Mater. Eng.* **2012**, *18*, 177–186.
108. Ohashi, O.; Kaieda, Y. Hot isostatic pressing of diffusion bonds in SUS 304 stainless steel. *Weld. Int.* **1990**, *4*, 35–41. [[CrossRef](#)]
109. Gietzelt, T.; Toth, V.; Huell, A. Diffusion Bonding: Influence of Process Parameters and Material Microstructure. *Join. Technol.* **2016**. [[CrossRef](#)]
110. Ogawa, K.; Azuma, S. Intergranular corrosion resistance of stainless steel diffusion-bonded joints with B-containing amorphous insert metal. *Weld. Int.* **1995**, *9*, 440–445. [[CrossRef](#)]
111. Harumoto, T.; Yamashita, Y.; Ohashi, O.; Ishiguro, T. Influence of Cold Rolling on Diffusion Bondability of SUS316L Stainless Steel Sheets. *Mater. Trans.* **2014**, *55*, 633–636. [[CrossRef](#)]
112. Li, S.; Xuan, F.; Tu, S. In situ observation of interfacial fatigue crack growth in diffusion bonded joints of austenitic stainless steel. *J. Nucl. Mater.* **2007**, *366*, 1–7. [[CrossRef](#)]
113. Yeh, M.S.; Chuang, T.H. Low-pressure diffusion bonding of SAE 316 stainless steel by inserting a superplastic interlayer. *Scr. Metall. Mater.* **1995**, *33*, 1277–1281. [[CrossRef](#)]
114. Li, S.; Xuan, F.; Tu, S.; Yu, S. Microstructure evolution and interfacial failure mechanism in 316LSS diffusion-bonded joints. *Mater. Sci. Eng. A* **2008**, *491*, 488–491. [[CrossRef](#)]
115. Mateus, L.B.; George, G.; Nuernberg, V.; Henriques, M.; Mantelli, B. 316L Stainless Steel Diffusion Bonding Optimized Parameters. In Proceedings of the COBEM 2017, Curitiba, Brazil, 3–8 December 2017.
116. Shirzadi, A.A.; Kocak, M.; Wallach, E.R. Joining stainless steel metal foams. *Sci. Technol. Weld. Join.* **2004**, *9*, 277–279. [[CrossRef](#)]
117. Martin, P.; Matson, D.; Bennett, W. Microfabrication Methods for Microchannel Reactors and Separations Systems. *Chem. Eng. Commun.* **1999**, *173*, 245–254. [[CrossRef](#)]
118. Yusa, N.; Hashizume, H. Fabrication of imitative stress corrosion cracking specimen using lithography and solid state bonding. *Int. J. Appl. Electromagn. Mech.* **2012**, *39*, 291–296. [[CrossRef](#)]
119. Tiwari, S.; Paul, B. Application of Nickel Nanoparticles in Diffusion Bonding of Stainless Steel Surfaces. In Proceedings of the MSEC2008, Evanston, IL, USA, 7–10 October 2008; pp. 1–6.
120. Tiwari, S.; Paul, B. Comparison of Nickel Nanoparticle-Assisted Diffusion Brazing of Stainless Steel to Conventional Diffusion Brazing and Bonding Processes. *J. Manuf. Sci. Eng.* **2010**, *132*, 1–5. [[CrossRef](#)]
121. Kim, S.H.; Cha, J.-H.; Jang, C.; Sah, I. Microstructure and Tensile Properties of Diffusion Bonded Austenitic Fe-Base Alloys—Before and After Exposure to High Temperature Supercritical-CO₂. *Metals* **2020**, *10*, 480. [[CrossRef](#)]
122. An, Z.; Luan, W.; Xuan, F.; Tu, S. High Temperature Performance of 316L-SS Joint Produced by Diffusion Bonding. *Key Eng. Mater.* **2005**, *300*, 2795–2799. [[CrossRef](#)]
123. Crockett, M.; Lane, J.W.; Kirchoff, V.; Josephson, M.E.; Gao, H.P.; Manjunath, B. Method of Diffusion Bonding a fluid flow apparatus. US Patent 7,798,388 B2, 21 September 2010.
124. Li, S.; Li, L.; Yu, S.; Akid, R.; Xia, H. Investigation of intergranular corrosion of 316L stainless steel diffusion bonded joint by electrochemical potentiokinetic reactivation. *Corros. Sci.* **2011**, *53*, 99–104. [[CrossRef](#)]
125. Li, S.; Xuan, F.; Tu, S. Fatigue damage of stainless steel diffusion-bonded joints. *Mater. Sci. Eng. A* **2008**, *480*, 125–129. [[CrossRef](#)]
126. Veiga, C.; Davim, J.; Loureiro, A. Properties and applications of titanium alloys: A brief review. *Rev. Adv. Mater. Sci.* **2012**, *32*, 14–34.
127. Kundu, S.; Chatterjee, S. Interface microstructure and strength properties of diffusion bonded joints of titanium-Al interlayer-18Cr-8Ni stainless steel. *Mater. Sci. Eng. A* **2010**, *527*, 2714–2719. [[CrossRef](#)]
128. Yang, G.; Ma, D.; Liu, L.; Rong, J.; Yu, X. Thermal Diffusion Bonding of Pure Titanium to 304 Stainless Steel Using Aluminum Interlayer. *Chem. Eng. Trans.* **2017**, *59*, 1045–1050.
129. Bhanumurthy, K.; Kale, G. Reactive diffusion between titanium and stainless steel. *J. Mater. Sci. Lett.* **1993**, *12*, 1879–1881. [[CrossRef](#)]

130. Ananthakumar, K.; Kumaran, S. Experimental Investigation and Prediction of Optimum Process Parameter for Plasma Assisted Diffusion Bonding of Commercial Pure Titanium and Austenitic Stainless Steel. *Arab. J. Sci. Eng.* **2019**, *44*, 1017–1032. [[CrossRef](#)]
131. Alemán, B.; Gutiérrez, L.; Urcola, J. Interface microstructures in diffusion bonding of titanium alloys to stainless and low alloy steels. *Mater. Sci. Technol.* **1993**, *9*, 633–641. [[CrossRef](#)]
132. Ghosh, M.; Laik, A.; Bhanumurthy, K.; Kale, G.B.; Krishnan, J.; Chatterjee, S. Evolution of interface microstructure and strength properties in titanium-Stainless steel diffusion bonded transition joints. *Mater. Sci. Technol. Dec.* **2004**, *20*, 1578–1584. [[CrossRef](#)]
133. Shirzadi, A.A.; Laik, A.; Tewari, R.; Orsborn, J.; Dey, G.K. Materialia Gallium-assisted diffusion bonding of stainless steel to titanium; microstructural evolution and bond strength. *Materialia* **2018**, *4*, 115–126. [[CrossRef](#)]
134. Deng, Y.; Sheng, G.; Xu, C. Evaluation of the microstructure and mechanical properties of diffusion bonded joints of titanium to stainless steel with a pure silver interlayer. *Mater. Des.* **2013**, *46*, 84–87. [[CrossRef](#)]
135. Deng, Y.Q.; Sheng, G.M.; Huang, Z.H.; Fan, L.Z. Microstructure and mechanical properties of diffusion bonded titanium/304 stainless steel joint with pure Ag interlayer. *Sci. Technol. Weld. Join.* **2013**, *18*, 143–147. [[CrossRef](#)]
136. Jie, W.; Yang, F.; Hao, L.; Jin, Y.; Haotian, Y.; Fuqi, Z. Microstructure and mechanical properties of TC4/0Cr18Ni9 joint prepared by transient liquid phase diffusion bonding. *Mater. Res. Express* **2019**, *6*, 1065d6. [[CrossRef](#)]
137. Ghosh, M.; Bhanumurthy, K.; Kale, G.B. Diffusion bonding of titanium to 304 stainless steel. *J. Nucl. Mater.* **2003**, *322*, 235–241. [[CrossRef](#)]
138. Li, J.; Huo, L.; Zhang, F.; Xiong, J.; Li, W. Fracture Characteristics of Vacuum Diffusion Bonded TA2 Titanium to 1Cr18Ni9Ti Stainless Steel Joint with Nb + Ni Interlayers. *Mater. Sci. Forum* **2009**, *622*, 399–402. [[CrossRef](#)]
139. Kundu, S.; Chatterjee, S. Evolution of Interface Microstructure and Mechanical Properties of Titanium/304 Stainless Steel Diffusion Bonded Joint Using Nb Interlayer. *ISIJ Int.* **2010**, *50*, 1460–1465. [[CrossRef](#)]
140. Szwed, B.; Konieczny, M. Structural changes during the formation of diffusion bonded joints between titanium and stainless steel. *IOP Conf. Ser. Mater. Sci. Eng.* **2018**, *461*, 012082. [[CrossRef](#)]
141. Szwed, B.; Konieczny, M. Microstructure and Mechanical Properties of Joints of Titanium with Stainless Steel Performed using Nickel Filler. *Arch. Met. Mater.* **2016**, *61*, 997–1001. [[CrossRef](#)]
142. Kundu, S.; Chatterjee, S. Interfacial microstructure and mechanical properties of diffusion-bonded titanium-stainless steel joints using a nickel interlayer. *Mater. Sci. Eng. A* **2006**, *425*, 107–113. [[CrossRef](#)]
143. Kundu, S.; Chatterjee, S. Effect of Reaction Products on Mechanical Properties of Diffusion Bonded of Titanium to 304 Stainless Steel with Cu Interlayer Joints. *Trans. Indian Inst. Met.* **2008**, *61*, 457–464. [[CrossRef](#)]
144. Kundu, S.; Ghosh, M.; Laik, A.; Bhanumurthy, K.; Kale, G.B.; Chatterjee, S. Diffusion bonding of commercially pure titanium to 304 stainless steel using copper interlayer. *Mater. Sci. Eng. A* **2005**, *407*, 154–160. [[CrossRef](#)]
145. Kundu, S.; Chatterjee, S. Effects of temperature on interface microstructure and strength properties of titanium-Niobium stainless steel diffusion bonded joints. *Mater. Sci. Technol.* **2011**, *27*, 1177–1182. [[CrossRef](#)]
146. Akbar, A.; Mahdi, B.; Aluwi, A. Characterization of Diffusion Bonding of Stainless Steel AISI 316 and Pure Titanium sheets Using Copper Interlayer. *IOP Conf. Ser. Mater. Sci. Eng.* **2019**, *518*, 032041. [[CrossRef](#)]
147. Ghosh, M.; Kundu, S.; Chatterjee, S.; Mishra, B. Influence of Interface Microstructure on the Strength of the Transition Joint between Ti-6Al-4V and Stainless Steel. *Metall. Mater. Trans. A* **2005**, *36*, 1891–1899. [[CrossRef](#)]
148. Chandrappa, K.; Kumar, A.; Shubham, K. Diffusion bonding of a titanium alloy to a stainless steel with an aluminium alloy interlayer. *IOP Conf. Ser. Mater. Sci. Eng.* **2018**, *402*, 012124. [[CrossRef](#)]
149. Alhazaa, A.; Khan, T.I.; Haq, I. Transient liquid phase (TLP) bonding of Al7075 to Ti-6Al-4V alloy. *Mater. Charact.* **2010**, *61*, 312–317. [[CrossRef](#)]
150. Alhazaa, A.N.; Khan, T.I. Diffusion bonding of Al7075 to Ti-6Al-4V using Cu coatings and Sn-3. 6Ag-1Cu interlayers. *J. Alloys Compd.* **2010**, *494*, 351–358. [[CrossRef](#)]
151. He, P.; Yue, X.; Zhang, J.H. Hot pressing diffusion bonding of a titanium alloy to a stainless steel with an aluminum alloy interlayer. *Mater. Sci. Eng. A* **2008**, *486*, 171–176. [[CrossRef](#)]
152. Habisch, S.; Peter, S.; Grund, T.; Mayr, P. The Effect of Interlayer Materials on the Joint Properties of Diffusion-Bonded Aluminium and Magnesium. *Metals* **2018**, *8*, 138. [[CrossRef](#)]
153. Thirunavukarasu, G.; Kundu, S.; Mishra, B. Effect of Bonding Temperature on Interfacial Reaction and Mechanical Properties of Diffusion-Bonded Joint Between Ti-6Al-4V and 304 Stainless Steel Using Nickel as an Intermediate Material. *Metall. Mater. Trans. A* **2014**, *45*, 2067–2077. [[CrossRef](#)]
154. Balasubramanian, M. Application of Box-Behnken design for fabrication of titanium alloy and 304 stainless steel joints with silver interlayer by diffusion bonding. *Mater. Des.* **2015**, *77*, 161–169. [[CrossRef](#)]

155. Balasubramanian, M. Characterization of diffusion-bonded titanium alloy and 304 stainless steel with Ag as an interlayer. *Int. J. Adv. Manuf. Technol.* **2016**, *82*, 153–162. [[CrossRef](#)]
156. He, P.; Zhang, J.; Li, X. Diffusion bonding of titanium alloy to stainless steel wire mesh. *Mater. Sci. Technol.* **2001**, *17*, 1158–1162. [[CrossRef](#)]
157. Thirunavukarasu, G.; Kundu, S.; Laha, T.; Roy, D.; Chatterjee, S. Exhibition of veiled features in diffusion bonding of titanium alloy and stainless steel via copper. *Metall. Res. Technol.* **2018**, *115*, 115. [[CrossRef](#)]
158. Balasubramanian, M. Development of processing windows for diffusion bonding of Ti-6Al-4V titanium alloy and 304 stainless steel with silver as intermediate layer. *Trans. Nonferrous Met. Soc. China* **2015**, *25*, 2932–2938. [[CrossRef](#)]
159. Özdemir, N.; Bilgin, B. Interfacial properties of diffusion bonded Ti-6Al-4V to AISI 304 stainless steel by inserting a Cu interlayer. *Int. J. Adv. Manuf. Technol.* **2009**, *41*, 519–526. [[CrossRef](#)]
160. Yang, L.; Jiang, X.; Sun, H.; Song, T.; Mo, D.; Li, X.; Luo, Z. Interfacial reaction and microstructure investigation of TC4/V/Cu/Co/316L diffusion-bonded joints. *Mater. Lett.* **2020**, *261*, 127140. [[CrossRef](#)]
161. Kurt, B.; Orhan, N.; Kaya, M. Interface characterisation of diffusion bonded Ti-6Al-4V alloy and austenitic stainless steel couple. *Mater. Sci. Technol.* **2009**, *25*, 556–560. [[CrossRef](#)]
162. Zakipour, S.; Halvae, A.; Ali, A.; Samavatian, M.; Khodabandeh, A. An investigation on microstructure evolution and mechanical properties during transient liquid phase bonding of stainless steel 316L to Ti-6Al-4V. *J. Alloys Compd.* **2015**, *626*, 269–276. [[CrossRef](#)]
163. Vigraman, T.; Ravindran, D.; Narayanasamy, R. Effect of phase transformation and intermetallic compounds on the microstructure and tensile strength properties of diffusion-bonded joints between Ti-6Al-4V and AISI 304L. *Mater. Des.* **2012**, *36*, 714–727. [[CrossRef](#)]
164. Negemiya, A.A.; Rajakumar, S.; Balasubramanian, V. High-temperature diffusion bonding of austenitic stainless steel to titanium dissimilar joints. *Mater. Res. Express* **2019**, *6*, 066572. [[CrossRef](#)]
165. Ferrante, M.; Pigoretti, E.V. De Diffusion bonding of Ti-6Al-4V to AISI 316L stainless steel: Mechanical resistance and interface microstructure. *J. Mater. Sci.* **2002**, *7*, 2825–2833. [[CrossRef](#)]
166. Norouzi, E.; Atapour, M.; Shamanian, M. Effect of bonding time on the joint properties of transient liquid phase bonding between Ti-6Al-4V and AISI 304. *J. Alloys Compd.* **2017**, *701*, 335–341. [[CrossRef](#)]
167. Norouzi, E.; Atapour, M.; Shamanian, M.; Allafchian, A. Effect of bonding temperature on the microstructure and mechanical properties of Ti-6Al-4V to AISI 304 transient liquid phase bonded joint. *Mater. Des.* **2016**, *99*, 543–551. [[CrossRef](#)]
168. Surendar, A.; Lucas, A.; Abbas, M.; Rahim, R.; Salmani, M. Transient liquid phase bonding of stainless steel 316 L to Ti-6Al-4 V using Cu/Ni multi-interlayer: Microstructure, mechanical properties, and fractography. *Weld. World* **2019**, *63*, 1025–1032. [[CrossRef](#)]
169. Zakipour, S.; Samavatian, M.; Halvae, A.; Amadeh, A.; Khodabandeh, A. The effect of interlayer thickness on liquid state diffusion bonding behavior of dissimilar stainless steel 316/Ti-6Al-4V system. *Mater. Lett.* **2015**, *142*, 168–171. [[CrossRef](#)]
170. Akbar, A.; Ajeel, S.; Hassoni, S. Optimization of Diffusion Bonding of Pure Copper (OFHC) with Stainless Steel 304L. *Al-Khwarizmi Eng. J.* **2018**, *14*, 30–39. [[CrossRef](#)]
171. Yilmaz, O. Effect of welding parameters on diffusion bonding of type 304 stainless steel-Copper bimetal. *Mater. Sci. Technol.* **2001**, *17*, 989–994. [[CrossRef](#)]
172. Kaya, Y.; Kahraman, N.; Durgutlu, A.; Güle, B. A novel approach to diffusion bonding of copper to stainless steel. *Proc. Inst. Mech. Eng. Part B J. Eng. Manuf.* **2011**, *226*, 478–484. [[CrossRef](#)]
173. Xiong, J.; Xie, Q.; Li, J.; Zhang, F.; Huang, W. Diffusion Bonding of Stainless Steel to Copper with Tin Bronze and Gold Interlayers. *J. Mater. Eng. Perform.* **2012**, *21*, 33–37. [[CrossRef](#)]
174. Sabharwall, P.; Clark, D.E.; Mizia, R.E.; Glazoff, M.V.; Mckellar, M.G. Diffusion-Welded Microchannel Heat Exchanger for Industrial Processes. *J. Therm. Sci. Eng. Appl.* **2013**, *5*, 011009. [[CrossRef](#)]
175. Wang, S.; Zhang, M.; Wu, H.; Yang, B. Materials Characterization Study on the dynamic recrystallization model and mechanism of nuclear grade 316LN austenitic stainless steel. *Mater. Charact.* **2016**, *118*, 92–101. [[CrossRef](#)]
176. Uhs, U.; Zhang, C.; Bellet, M.; Bobadilla, M.; Shen, H. A Coupled Electrical-Thermal-Mechanical Modeling of Gleeble Tensile Tests for Ultra-High-Strength (UHS) Steel at a High Temperature. *Metall. Mater. Trans. A* **2010**, *41*, 2304–2317.

177. Luo, J.; Chen, B.; Yuan, Q.; Zhang, D.F. Effect of heating-rate on failure temperature of pre-loaded magnesium alloy. *Trans. Nonferrous Met. Soc. China* **2010**, *20*, S371–S375. [[CrossRef](#)]
178. Kheder, A.; Akbar, A.; Jubeh, N. Diffusion welding of OFHC copper to austenitic stainless steel 316L. *Int. J. Join. Mater.* **2004**, *16*, 97–102.
179. Nishi, H.; Araki, T.; Eto, M. Diffusion bonding of alumina dispersion-strengthened copper to 316 stainless steel with interlayer metals. *Fusion Eng. Des.* **1998**, *40*, 505–511. [[CrossRef](#)]
180. Krishnan, J.; Bhanumurthy, K.; Gawde, P.; Derose, J.; Kale, G.; Srikrushnamurthy, G. Manufacture of a matrix heat exchanger by diffusion bonding. *J. Mater. Process. Technol.* **1997**, *66*, 85–89. [[CrossRef](#)]
181. Batra, I.S.; Kale, G.B.; Saha, T.K.; Ray, A.K.; Derose, J.; Krishnan, J. Diffusion bonding of a Cu–Cr–Zr alloy to stainless steel and tungsten using nickel as an interlayer. *Mater. Sci. Eng. A* **2004**, *369*, 119–123. [[CrossRef](#)]
182. Nishi, H.; Araki, T. Low cycle fatigue strength of diffusion bonded joints of alumina dispersion-strengthened copper to stainless steel. *J. Nucl. Mater.* **2000**, *287*, 1234–1237. [[CrossRef](#)]
183. Nishi, H. Notch toughness evaluation of diffusion-bonded joint of alumina dispersion-strengthened copper to stainless steel. *Fusion Eng. Des.* **2006**, *81*, 269–274. [[CrossRef](#)]
184. Singh, K.P.; Patel, A.; Bhoje, K.; Khirwadkar, S.S.; Mehta, M. Optimization of the diffusion bonding parameters for SS316L/CuCrZr with and without Nickel interlayer. *Fusion Eng. Des.* **2016**, *112*, 274–282. [[CrossRef](#)]
185. Nishi, H.; Muto, Y.; Sato, K. Solid-state diffusion bonding of alumina dispersion-strengthened copper to 316 stainless steel. *J. Nucl. Mater.* **1994**, *5*, 1585–1589. [[CrossRef](#)]
186. Banerjee, S.; Banerjee, M. Nuclear Applications: Zirconium Alloys. *Ref. Modul. Mater. Sci. Mater. Eng.* **2016**, 1–15. [[CrossRef](#)]
187. Yagnik, S.; Garde, A. Zirconium Alloys for LWR Fuel Cladding and Core Internals. In *Structural Alloys for Nuclear Energy Applications*; Elsevier Inc: Amsterdam, The Netherlands, 2019; pp. 247–291, ISBN 9780123970466.
188. Matweb Zirconium Alloy. Available online: <http://www.matweb.com/search/datasheettext.aspx?matguid=eb1dad5ce1ad4a1f9e92f86d5b44740d> (accessed on 24 April 2020).
189. Bhanumurthy, K.; Krishnan, J.; Kale, G.B.; Banerjee, S. Transition joints between Zircaloy-2 and stainless steel by diffusion bonding. *J. Nucl. Mater.* **1994**, *217*, 67–74. [[CrossRef](#)]
190. Pan, H.; Liu, B.; Guo, Y.; Liu, Y.; Quan, G. An investigation on diffusion bonding of Zircaloy-4 and 304L stainless steel with Ti and Ag multiple interlayers. *Mater. Lett.* **2019**, *240*, 185–188. [[CrossRef](#)]
191. Srikanth, V.; Laik, A.; Dey, G.K. Materials & Design Joining of stainless steel 304L with Zircaloy-4 by diffusion bonding technique using Ni and Ti interlayers. *Mater. Des.* **2017**, *126*, 141–154.
192. Abdelatif, L.; Taouinet, M.; Soltane, L. Microstructural Aspects of the Zircaloy-4/SS-304L Interface Obtained by Diffusion Bonding Technique. *Solid State Phenom.* **2019**, *297*, 17–30.
193. Taouinet, M.; Lebaili, S.; Souami, N. Characterization of the interface to diffusion bonding of zircaloy-4 and stainless steel. *Phys. Procedia* **2009**, *2*, 1231–1239. [[CrossRef](#)]
194. Zaid, B.; Taouinet, M.; Souami, N.; Lebaili, S. Microstructure and Corrosion Aspects of Dissimilar Joints of Zircaloy-4 and 304L Stainless Steel. *J. Mater. Eng. Perform.* **2013**, *22*, 854–862. [[CrossRef](#)]
195. Lebaili, A.; Lebaili, S.; Hodaj, F. Interfacial interactions between 304L stainless steel and Zy-4 alloy during isothermal holdings at 1050 C. *J. Alloys Compd.* **2019**, *805*, 565–577. [[CrossRef](#)]
196. Taouinet, M.; Kamel, N.E.; Lebaili, S. Diffusion Bonding Between Zircaloy-4 and 304L Stainless Steel in the Presence of a Eutectic. *Mater. Manuf. Process.* **2013**, *28*, 1327–1334. [[CrossRef](#)]
197. Lebaili, A.; Taouinet, M.; Nibou, D.; Lebaili, S.; Hodaj, F. Effect of Isothermal Hold on the Microstructural Evolution of the Stainless Steel 304L/Zircaloy-4 Interface. *J. Mater. Eng. Perform.* **2017**, *26*, 3112–3120. [[CrossRef](#)]
198. Aboudi, D.; Lebaili, S.; Taouinet, M.; Zollinger, J. Microstructure evolution of diffusion welded 304L/Zircaloy 4 with copper interlayer. *Mater. Des.* **2017**, *116*, 386–394. [[CrossRef](#)]
199. Chen, H.; Long, C.; Wei, T.; Gao, W.; Xiao, H.; Chen, L. Effect of Ni interlayer on partial transient liquid phase bonding of Zr–Sn–Nb alloy and 304 stainless steel. *J. Mater. Des.* **2014**, *60*, 358–362. [[CrossRef](#)]
200. Lucuta, P.; Patru, I.; Visiliiu, F. Microstructural features of hot pressure bonding between stainless steel type AISI-304L and Zircaloy-2. *J. Nucl. Mater.* **1981**, *99*, 154–164. [[CrossRef](#)]
201. Ahmad, M.; Akhter, J.I.; Zaman, Q.; Shaikh, M.A.; Akhtar, M.; Iqbal, M.; Ahmed, E. Diffusion bonding of stainless steel to Zircaloy-4 in the presence of a Ta intermediate layer. *J. Nucl. Mater.* **2003**, *317*, 212–216. [[CrossRef](#)]
202. YHang, Y.; Feng, D.; He, Z.; Chen, X. Main Joining Methods of Ceramic and Metal. *J. Iron Steel Res.* **2006**, *13*, 1–5.

203. Akselsen, O. Review Diffusion bonding of ceramics. *J. Mater. Sci.* **1992**, *27*, 569–579. [[CrossRef](#)]
204. Mehrzad, M.; Sadeghi, A.; Farahani, M. Microstructure and properties of transient liquid phase bonding of AM60 Mg alloy to 304 stainless steel with Zn interlayer. *J. Mater. Process. Tech.* **2019**, *266*, 558–568. [[CrossRef](#)]
205. Elthalabawy, W.; Khan, T. Diffusion Bonding of Austenitic Stainless Steel 316L to a Magnesium Alloy. *Key Eng. Mater.* **2018**, *442*, 26–33. [[CrossRef](#)]
206. Elthalabawy, W.M.; Khan, T.I. Microstructural development of diffusion-brazed austenitic stainless steel to magnesium alloy using a nickel interlayer. *Mater. Charact.* **2010**, *61*, 703–712. [[CrossRef](#)]
207. Elthalabawy, W.; Khan, T. Liquid Phase Bonding of 316L Stainless Steel to AZ31 Magnesium Alloy. *J. Mater. Sci. Technol.* **2011**, *27*, 22–28. [[CrossRef](#)]
208. Shushan, S.; Charles, E.; Congleton, J. The Environment Assisted Cracking of Diffusion Bonded Stainless to Carbon Steel Joints in an Aqueous Chloride Solution. *Corros. Sci.* **1996**, *38*, 4–9. [[CrossRef](#)]
209. Bhanumurthy, K.; Derose, D.J.; Kale, G.B.; Krishnan, J. Solid state bonding of porous nickel electrode to AISI 304 austenitic stainless steel. *Mater. Sci. Technol.* **2004**, *20*, 1059–1063. [[CrossRef](#)]
210. Aleman, B.; Gutierrez, I.; Urcola, J.J. The use of Kirkendall effect for calculating intrinsic diffusion coefficients in a 316L/Ti6242 diffusion bonded couple. *Scr. Mater.* **1997**, *36*. [[CrossRef](#)]
211. Abdolvand, R.; Atapour, M.; Shamanian, M.; Allafchian, A. The effect of bonding time on the microstructure and mechanical properties of transient liquid phase bonding between SAF 2507. *J. Manuf. Process.* **2017**, *25*, 172–180. [[CrossRef](#)]
212. Moravec, J.; Novakova, I. The Selection of Appropriate Process Parameters of Diffusion Bonding in Heterogeneous Weld of 355J2/AISI 316L Steels. *Key Eng. Mater.* **2017**, *737*, 101–106. [[CrossRef](#)]
213. Kurt, B.; Eroglu, M. Diffusion bonding between high chromium white iron and austenitic stainless steel. *Sci. Technol. Weld. Join.* **2007**, *12*, 467–472. [[CrossRef](#)]
214. Song, T.; Jiang, X.; Shao, Z.; Mo, D.; Zhu, D.; Zhu, M. The Interfacial Microstructure and Mechanical Properties of Diffusion-Bonded Joints of 316L Stainless Steel and the 4J29 Kovar Alloy Using Nickel as an Interlayer. *Metals* **2016**, *6*, 263. [[CrossRef](#)]
215. Fang, Y.J.; Jiang, X.S.; Mo, D.F.; Song, T.F.; Luo, Z.P. Microstructure and mechanical properties of the vacuum diffusion bonding joints of 4J29 kovar alloy and 316L stainless steel using pure cobalt interlayer. *Vacuum* **2019**, *168*, 108847. [[CrossRef](#)]
216. Travessa, D.; Ferrante, M.; den Ouden, G. Diffusion bonding of aluminium oxide to stainless steel using stress relief interlayers. *Mater. Sci. Eng. A* **2002**, *337*, 287–296. [[CrossRef](#)]
217. Kliauga, A.M.; Travessa, D.; Ferrante, M. Al₂O₃/Ti interlayer/AISI 304 diffusion bonded joint Microstructural characterization of the two interfaces. *Mater. Charact.* **2001**, *46*, 65–74. [[CrossRef](#)]
218. Torun, O.; Celikyurek, I. Microstructure and strength of diffusion-bonded joint between nickel aluminide Ni75Al25 and AISI 316 L stainless steel using a nickel interlayer. *Kov. Mater.* **2009**, *47*, 263–267.
219. Çalik, A. Interface microstructure of diffusion bonded Ni₃Al intermetallic alloy and austenitic stainless steel. *Mater. Lett.* **2009**, *63*, 2462–2465. [[CrossRef](#)]
220. Stoop, B.; Den Ouden, G. Diffusion Bonding of Silicon Nitride to Austenitic Stainless Steel with Metallic Interlayers. *Metall. Mater. Trans. A Phys. Metall. Mater. Sci.* **1995**, *26*, 203–208. [[CrossRef](#)]
221. Polanco, R.; Pablos, A.; Miranzo, P.; Osendi, M.I. Metal—Ceramic interfaces: Joining silicon nitride—Stainless steel. *Appl. Surf. Sci.* **2004**, *238*, 506–512. [[CrossRef](#)]
222. Hussain, P.; Mamat, O.; Mohammad, M.; Jaafar, W. Formation of Nitrogen-Pearlite in the Diffusion Bonding of Sialon to 316L Stainless. *AIP Conf. Proc.* **2010**, *2007*, 129–134.
223. Hussain, P.; Isnin, A. Joining of austenitic stainless steel and ferritic stainless steel to sialon. *J. Mater. Process. Technol.* **2001**, *113*, 222–227. [[CrossRef](#)]
224. Jia, L.; Guangmin, S.; Li, H. Ti-Nb-Cu Stress Buffer Layer for TiC Cermet/304 Stainless Steel Diffusion Bonding. *Rare Met. Mater. Eng.* **2016**, *45*, 555–560.
225. Yönetken, A.; Cakmakkaya, M.; Erol, A.; Talas, S. Diffusion Bonding of Electroless Ni plated WC composite to Cu and AISI 316 Stainless Steel. *Mater. Sci.* **2011**, *29*, 15–21. [[CrossRef](#)]
226. Vegter, R.; den Ouden, G. The Influence of Residual Stresses on the Mechanical Behaviour of ZrO₂ Ni AISI 316 Diffusion Bonds. *Mater. Sci. Forum* **2000**, *349*, 634–639. [[CrossRef](#)]
227. Qin, C.; Derby, B. Diffusion Bonds between a Stainless Steel and Zirconia. *J. Am. Ceram. Soc.* **1993**, *76*, 232–234. [[CrossRef](#)]
228. Loh, N.L.; Sia, K.Y. An overview of hot isostatic pressing. *J. Mater. Process. Technol.* **1992**, *30*, 45–65. [[CrossRef](#)]

229. Atkinson, H.V.; Davies, S. Fundamental Aspects of Hot Isostatic Pressing: An Overview. *Metall. Mater. Trans. A* **2000**, *31*, 2981–3000. [[CrossRef](#)]
230. Bocanegra-Bernal, M. Hot Isostatic Pressing (HIP) technology and its applications to metals and ceramics. *J. Mater. Sci.* **2004**, *9*, 6399–6420. [[CrossRef](#)]
231. Lipa, M.; Durocher, A.; Tivey, R.; Huber, T.; Schedler, B.; Weigert, J. The use of copper alloy CuCrZr as a structural material for actively cooled plasma facing and in vessel components. *Fusion Eng. Des.* **2005**, *79*, 469–473. [[CrossRef](#)]
232. Yamada, T.; Noto, H.; Hishinuma, Y.; Muroga, T.; Nakamura, H. Development of a dispersion strengthened copper alloy using a MA-HIP method. *Nucl. Mater. Energy* **2016**, *9*, 455–458. [[CrossRef](#)]
233. Wei, R.; Li, Q.; Wang, W.J.; Wang, J.C.; Wang, X.L.; Xie, C.Y.; Luo, G. Microstructure and properties of W-Cu/CuCrZr/316L joint bonded by one-step HIP technique. *Fusion Eng. Des.* **2018**, *128*, 47–52. [[CrossRef](#)]
234. Wikman, S.; Peacock, A.; Zlamal, O.; Öijerholm, J.; Tähtinen, S.; Rödiger, M.; Marmy, P.; Gillia, O.; Lorenzetto, P.; Heikkinen, S. Assessment of materials data for blanket materials within the European contribution to ITER. *J. Nucl. Mater.* **2013**, *442*, S414–S419. [[CrossRef](#)]
235. Wei, R.; Zhao, S.X.; Dong, H.; Che, H.Y.; Li, Q.; Wang, W.J.; Wang, J.C.; Wang, X.L.; Sun, Z.X.; Luo, G. Enhancing the CuCrZr/316L HIP-joint by Ni electroplating. *Fusion Eng. Des.* **2017**, *117*, 58–62. [[CrossRef](#)]
236. Goods, S.H.; Puskar, J.D. Solid state bonding of CuCrZr to 316L stainless steel for ITER applications. *Fusion Eng. Des.* **2011**, *86*, 1634–1638. [[CrossRef](#)]
237. Frayssines, P.; Bucci, P.; Vito, E.; Rigal, E.; Lorenzetto, P. Cleaning surface treatments for the fabrication of ITER First Wall panels by HIP. *J. Nucl. Mater.* **2009**, *386*, 866–870. [[CrossRef](#)]
238. Sato, S.; Hatano, T.; Kuroda, T.; Furuya, K.; Hara, S.; Enoeda, M.; Takatsu, H. Optimization of HIP bonding conditions for ITER shielding blanket/First wall made from austenitic stainless steel and dispersion strengthened copper alloy. *J. Nucl. Mater.* **1998**, *263*, 265–270. [[CrossRef](#)]
239. Sato, S.; Kuroda, T.; Kurasawa, T.; Furuya, K.; Togami, I.; Takatsu, H. Mechanical properties of HIP bonded joints of austenitic stainless steel and Cu-alloy for fusion experimental reactor blanket. *J. Nucl. Mater.* **1996**, *237*, 940–944. [[CrossRef](#)]
240. Sato, S.; Kuroda, T.; Hatano, T.; Furuya, K.; Tokami, I.; Takatsu, H. Development of first wall/blanket structure by hot isostatic pressing (HIP) in the JAERI. *Fusion Eng. Des.* **1998**, *40*, 609–614. [[CrossRef](#)]
241. Hatano, T.; Saito, M.; Enoeda, M.; Takatsu, H. Fracture strengths of HIPed DS-Cu/SS joints for ITER shielding blanket/First wall. *J. Nucl. Mater.* **1998**, *263*, 950–954. [[CrossRef](#)]
242. Marois, G.; Burlet, H.; Solomon, R.; Marini, B.; Gentzbittel, J.M. Structural materials joints for ITER in-vessel components. *Fusion Eng. Des.* **1998**, *40*, 253–261. [[CrossRef](#)]
243. Marois Le, G.; Dellis, C.; Gentzbittel, J.M.; Moret, F. HIP'ing of copper alloys to stainless steel. *J. Nucl. Mater.* **1996**, *237*, 927–931. [[CrossRef](#)]
244. Wang, J.; Wang, W.; Wei, R.; Wang, X.; Sun, Z.; Xie, C.; Li, Q.; Luo, G. Effect of Ti interlayer on the bonding quality of W and steel HIP joint. *J. Nucl. Mater.* **2017**, *485*, 8–14. [[CrossRef](#)]
245. Zhang, J.; Xie, D.; Li, Q.; Jiang, C.; Li, Q. Effect of holding time on the microstructure and strength of tungsten/steel joints by HIP diffusion bonded using a Cu interlayer. *Mater. Lett.* **2020**, *261*, 126875. [[CrossRef](#)]
246. JWS, I.G. *Material Assessment Report (MAR)*; G A1 DDD 1 98-05-28 W0.3; TER: Garching, Germany, 1998.

